J. Math. Biol. (2013) 66:1409–1462
DOI 10.1007/s00285-012-0539-4

Mathematical Biology

A review of spatial computational models for multi-cellular systems, with regard to intestinal crypts and colorectal cancer development

Giovanni De Matteis · Alex Graudenzi · Marco Antoniotti

Received: 25 July 2011 / Revised: 11 April 2012 / Published online: 8 May 2012

Abstract Colon rectal cancers (CRC) are the result of sequences of mutations which lead the intestinal tissue to develop in a carcinoma following a "progression" of observable phenotypes. The actual modeling and simulation of the key biological structures involved in this process is of interest to biologists and physicians and, at the same time, it poses significant challenges from the mathematics and computer science viewpoints. In this report we give an overview of some mathematical models for cell sorting (a basic phenomenon that underlies several dynamical processes in an organism), intestinal crypt dynamics and related problems and open questions. In particular, major attention is devoted to the survey of so-called *in-lattice* (or *grid*) models and *off-lattice* (*off-grid*) models. The current work is the groundwork for future research on semi-automated hypotheses formation and testing about the behavior of the various actors taking part in the adenoma–carcinoma progression, from regulatory processes to cell–cell signaling pathways.

Keywords Cell sorting · Crypt dynamics · Colorectal cancer · Cell adhesion · Modeling · Simulation

This work has been supported by Regione Lombardia under the research project RETRONET through the grant 12-4-5148000-40; U.A 053.

G. De Matteis
Department of Mathematics "F. Enriques", University of Milan, Via Saldini 50, 20133 Milan, Italy
e-mail: giovanni.dematteis@unimi.it

A. Graudenzi (✉) · M. Antoniotti
Department of Informatics, Systems and Communication, University of Milan Bicocca,
Viale Sarca 336, 20126 Milan, Italy
e-mail: alex.graudenzi@unimib.it

M. Antoniotti
e-mail: marco.antoniotti@unimib.it

Mathematics Subject Classification MSC 37N25 · MSC 92-08 · MSC 92B05 · MSC 92C15 · MSC 92C17 · MSC 92C42

Contents

1 Introduction

Systems biology is an emerging new field of science, addressing the complexity of biology from molecular scales to ecosystems and explaining phenomena as they *emerge* from the interactions of numerous smaller components. Within this broad scientific framework we have focused our attention on the computational modeling of biological tissues, with the specific goal of uncovering the basic mechanisms and the general properties of cellular and intercellular dynamics. To this end a multicellular structure of particular interest is the *colonic crypt*, since this is the site in mammals where mutations in the epithelial stem cells, which are responsible for the gut lining renewal, may eventually steer a cell ensemble down the *adenoma–carcinoma* sequence, resulting in *Colorectal Cancer* (CRC).

While there have been many biochemical and clinical studies of CRC and the overall progression along the adenoma–carcinoma sequence has been quite well characterized, there has been, since the early 1980s, only a few attempts to use mathematical models and computer simulation to obtain other insights in its overall biology. At the time of this writing, the current status of computing power allows to run very complex simulation of deeply complex biochemical models in a rather reasonable time. Hence, it is not surprising that many researchers have now directed their attention toward the mathematical and computational models of colonic crypts and CRC development (and, of course, other relevant systems).

Given these premises, in this work we intend to present a review of what we consider the *state of the art* of these models, aiming at underlining the strong points and the possible limitations, highlighting the open questions and providing interesting insights for possible future research directions, with special regard to the biological characterization of such systems, on the one hand, and the advances in the computational modeling of multi-cellular systems, on the other. This should also be a starting point for the (ambitious) goal of designing a coherent and possibly extensive multi-scale model for the development of the colorectal cancer.

The paper is organized as follows. Section 2 is devoted to a biological introduction to the problem. Section 3 reports a list of the basic phenomena occurring in colonic crypt dynamics. Section 4 concerns a classification of the up-to-date mathematical and computational models of multi-cellular systems, with special regard to intestinal crypts and CRC development. In Sect. 5, the in-lattice models are reviewed in-depth and accompanied by some example simulations. Section 6 describes in detail the so-called off-lattice models. Section 7 presents a survey of the currently available libraries, repositories and software with regard to this subject. Section 8 contains some comments on the evaluation criteria of the reviewed models. Finally, Sect. 9 reports a summary and an outline of the future research directions.

2 The intestine biology: a quick overview

In order to correctly model the development of the colorectal cancer it is essential to describe the basic biology of the intestine, with particular regard to the intestinal crypts, which are supposed to be the locus in which tumors originate (Alberts et al. 2007; Barker et al. 2009; Medema and Vermulen 2011). In particular, the goal of systems biology-oriented computational modeling is to effectively describe the dynamical features, the generic properties of the system and to provide a coherent picture of the signaling pathways that ensure its correct development and homeostasis (Kitano 2001, 2002; Kaneko 2006).

2.1 Morphological and functional description

The human gut essentially performs two main tasks, i.e. the digestion of the food and the absorption of the nutrients, with the chief hurdle of preventing the absorptive cells from being digested (Alberts et al. 2007 and quoted references therein).

Populations of muscular, stromal and cuboidal epithelial cells compose the different compartments of the intestine. In particular, the lining of the small intestine is a single-layered (self-renewing) epithelium, which covers the surface of the *villi*, i.e. fingers-like projections into the intestinal lumen, and that of the *crypts of Lieberkühn*, i.e. invagination within the connective tissue; in the large intestine no villus, but only crypts are present. Some of the epithelial cells are deputed to absorptive or digestive tasks, some other to the production of protective mucus (Sancho et al. 2004 and further references therein).

We can list 5 types of cells in the crypts, starting from *stem cells*, which are characterized by the retention of an undifferentiated phenotype, the extensive replication pace, the self-maintenance and the continuous origination of multi-lineage differentiation. Stem cells give rise to a progeny that undergoes post-mitotic differentiation events and develop different functions for the tissue (Potten et al. 2009 and further references therein). In particular, intestinal crypts are characterized by the presence of four epithelial lineages: *enterocytes*, which perform both absorptive and digestive activity, secreting hydrolases; *Goblet cell*, which secretes mucus to protect the absorptive cell from digestion; *Paneth cell*, which perform defensive tasks by means of antimicrobial peptides and enzymes; *enteroendocrine* cells, which are composed of

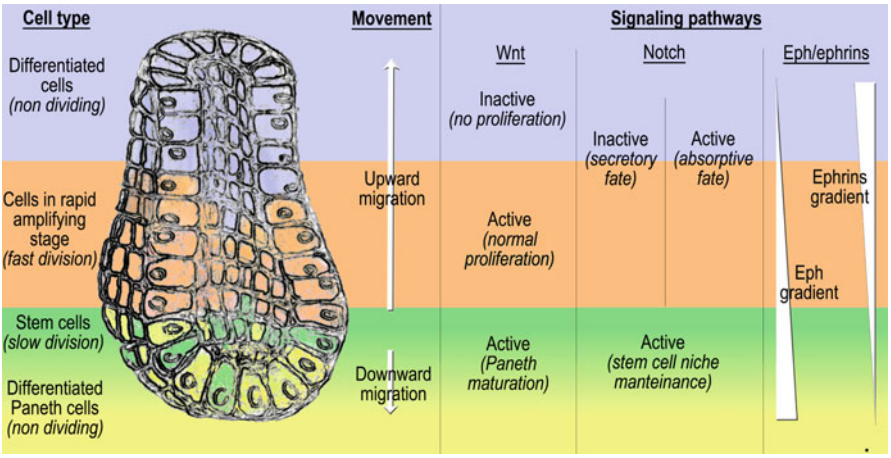

Fig. 1 A section of a crypt is represented, with specific regard to **a** the morphology, **b** the migration directions and **c** the signaling pathways involved in its dynamics and homeostasis. **a** In particular, we can distinguish four kinds of cells, starting from the bottom of the crypt, i.e. differentiated Paneth cells (*yellow*), stem cells (*green*), cells in rapid amplifying stage (*orange*) and differentiated (either absorptive or secretory) cells (*light blue*). **b** The migration direction is upward for all the cell types, exception made for stem cells that reside in a specific niche in the lower portion of the crypt and are intermingled with Paneth cells, which migrate downward. **c** The three main signaling pathways involved in the crypt dynamics are the Wnt pathway (its activation ensures the normal proliferation of the cells and the maturation of Paneth cells), the Notch signaling pathway (its activation ensures the maintenance of the stem cells niche, while for the other cell types its activation/inactivation drives cells toward either absorptive/secretory fates) and the Eph/ephrins pathway which regulates cell adhesion properties (color figure online)

15 subtypes and are involved in many different tasks and signaling pathways (Hocker and Wiedenmann 1998; Porter et al. 2002; Sancho et al. 2004).[1]

In regard to the spatial arrangement, the proliferative stem/progenitor compartments characterize the lower part of the crypt, while the differentiated cells reside at its top (exception made for the Paneth cells), as well as in the villus. Stem cells are sited at the bottom of the crypt in a specific niche, intermingled or just below Paneth cells (van Es et al. 2005) (see Fig. 1).

2.2 The dynamics

The epithelium of the intestinal crypts is a dynamic tissue characterized by a fast regeneration through cell growth, cell division, cell differentiation and apoptosis. To this end, spatial patterning and cell sorting are crucial processes in the tissue development and in order to segregate cell populations in distinct compartments characterized by different cell types and distinct functions (Alberts et al. 2007).

The overall dynamics of the crypt can be schematized as a coordinated upward migration of enterocyte, Goblet and enteroendocrine cells from the circumscribed

[1] Notice that besides the four main cell types, other cell types such as M-cells and Brush cells have been identified (van der Flier and Clevers 2009).

stem-cell region, which is in the lower region of the crypts, toward the top of the crypt, along the crypt-villus axis (Ratdke and Clevers 2005).

Stem cells generate progenies that enter a rapid proliferative phase and are maintained in a transit amplifying stage, continuing to divide and differentiate up to the final differentiated stage, when they undertake apoptosis and are finally shed into the intestinal lumen (the loss of cells is necessary to balance the production from the base of crypt). Paneth cells are the only cells that move downward and reside at the bottom of the crypt (Barker et al. 2009 and further references therein). On the other hand, the stem cell niche is maintained through a complex interplay of signaling pathways between the epithelial and the connective tissue (Potten et al. 2009). The coordinated positioning, the proliferation, the differentiation and the migration of the cells in the crypts are fundamental for the crypt homeostasis.

It is important to remark that the turnover process of the cells of the intestine is very fast: in mice the crypt progenitors divide every 12–16 h; in this way around 200–300 cells per crypt per day are generated and they successively undergo up to five rounds of cell division while migrating upwards. Accordingly, migrating cells travel from the base to the surface in about 3–6 days, while Paneth cells (which live for about 3–6 weeks) and stem cells localize at the crypt bottom and escape this flow (Marshman et al. 2002; Sancho et al. 2004; Frank 2007; Barker et al. 2009).

2.3 The signaling pathways

The signaling pathways throughout the epithelial cells and between the epithelium and the mesenchyme regulate many aspects of cellular activity, as the spatial patterning, the proliferation in transit-amplifying compartments, the commitment to specific lineages, the differentiation and the apoptosis (Sancho et al. 2004). Here we give a quick overview of three of the most important pathways involved in these processes.

2.3.1 Wnt signaling

Wnt signaling pathway is of fundamental importance in many developmental processes (Wodarz 1998; Logan and Nusse 2004; Reya and Clevers 2005). In regard to intestinal crypts, Wnt signaling is supposed to favor cell proliferation, establish the distinct modes of differentiation, avoid the immediate differentiation, and activate the expression of the Notch pathway (Sancho et al. 2004).[2]

[2] In detail, Beta-catenin is a cytoplasmic protein negatively regulated by the APC (Adenomatous Polyposis Coli) tumor suppressor complex. The activation of Wnt signals blocks the kinase activity of the APC complex, entailing the accumulation of Beta-catenin, which engages DNA-binding TCF/LFE proteins. Without Wnt signal these proteins repress the activation of specific genes, while in its presence they favor their activation. In proliferative cells inside the crypts there is an elevated accumulation of Beta-catenin, which hints to an important role of the Wnt signaling pathway in the proliferation of the intestinal progenitor cells (Kinzler and Vogelstein 1996; Bienz and Clevers 2000; Booth et al. 2002). Moreover, mutations of TCF/LEF or other Wnt inhibitions entail loss of the proliferative activity of the compartment, while the inhibition of beta-catenin/TCF4 activity in colorectal cancer cells induce changes in the cellular type (Korinek et al. 1998; Batlle et al. 2002; van de Wetering et al. 2002; Pinto et al. 2003).

In practice, while the activation of the Wnt signaling would keep the crypts in a normal proliferative state, ensuring the appropriate differentiation process, its absence entails the stop of the division/differentiation process, as it happens in the case of cells leaving the crypts. Notice also that in (Andreu et al. 2008; van Es et al. 2005) it is shown that the correct activation of Wnt pathway is required to determine Paneth cell fate and lineage, implying that this signaling pathway rules both a stem-cell/progenitor gene program and a Paneth cell maturation program.

It is important to mention that epithelial cells in the crypt produce both Wnt proteins and corresponding receptors, giving rise to a positive feedback loop (Alberts et al. 2007).

2.3.2 Notch signaling

Notch pathway is another key signaling pathway implicated in the development, the dynamics and the homeostasis of the crypt, through the control of the spatial patterning and the cell fate commitment, with the specific task of ensuring the status of undifferentiated proliferative cells in the progenitors compartment, in a concerted combination with the Wnt signals mechanism (Baron 2003).[3]

Summarizing, Notch signaling pathway mediates lateral inhibition, which forces the cells to diversify: some cells express Notch ligands and activate the Notch signaling in the neighbors, while avoiding their own activation: in this way they commit to the finally differentiated secretory fate; in the other cells the Notch ligands are inhibited while the Notch pathway is active within the cell itself: in this way they maintain the possibility of differentiating in any possible way. In both cases cells in transit amplifying stage continue dividing as long as they are in the crypts under the influence of the Wnt signals. When the Wnt signaling stops cells differentiate according to the state of the Notch activation, becoming absorptive if it is active, secretory if it is inactive. Therefore, the multi-potent crypt progenitors can be maintained only when both Wnt and Notch pathways are active.

Despite the lack of a conclusive theory describing the lineage specification from progenitors to fully differentiated cells, some interesting hypotheses and suggestions

[3] In detail, Notch genes synthesize large single trans-membrane receptors (Notch 1–4), correlated to five ligands (Delta-like 1,3 and 4, Jagged 1 and 2) (Mumm and Kopan 2000), involved in several processes linked to the cell fates. The interaction between Notch receptors and ligands provoke a proteolytic cleavage of the receptor close to the membrane, allowing the free Notch intracellular domain (NICD) to translocate within the nucleus where it activates the inhibitory transcription factor CSL (CBF1/RBPjk), usually correlated with the hairy/enhancer of split (HES) and the Achaete-Scute transcriptional repressors (involved in several transduction pathways and regulative mechanisms) (Mumm and Kopan 2000; Baron 2003).
Notch pathway controls the cell fate in adjacent cells in cluster of precursor cells, mediating the so-called *lateral inhibition* (Gierer and Meinhardt 1974; Meinhardt and Gierer 1974), which usually drives neighboring cells toward different fates. The proliferation/differentiation process, which is controlled by Wnt signaling pathway, is also influenced by the mechanism that underlies the cell fate determination: in this regard, Notch signaling is supposed to influence the several consecutive differentiation bifurcations (Schroder and Gossler 2002; Sancho et al. 2004).
The removal of a common Notch pathway transcription factor (i.e. CLS/RBP-J) entails a conversion of proliferative crypt cells in post-mitotic differentiated goblet cells (van Es et al. 2005; Alberts et al. 2007). On the other side, when the signaling pathway is activated no goblet cells are produced and the other dividing types of cell continue proliferating within the crypts.

have been put forth, as illustrated in van der Flier and Clevers (2009). Different signals appear to regulate the fates of the four principal cell types, according to a specific genetic hierarchy. In this regard, the Notch pathway seems to play a key function in the intestinal cell fate decisions.

2.3.3 Eph/Ephrin signaling

Eph/Ephrin bidirectional signaling is involved in numerous developmental processes, tissue patterning and cross-regulations in concert with other pathways (Arvanitis and Davy 2008 and quoted references therein).[4] The interaction between Eph receptors and ephrin ligands can trigger a downstream cascade that controls cell–cell adhesion, cell–substrate adhesion, cytoskeletal organization (Kullander and Klein 2002) and cell-extracellular matrix binding (Huynh-Do et al. 1999; Miao et al. 2000, 2005) influencing the formation and the stability of tight, adherence and gap junctions and integrin functions.[5]

Cell sorting is the process according to which population of cells tend to segregate and to form distinct compartments or different tissues (Xu et al. 1999; Poliakov et al. 2004). On the basis of the *Differential Adhesion Hypothesis*, *DAH*, Steinberg (1962), according to which cell sorting could be due to cell motility combined with differences in intercellular adhesiveness, tissue patterning and coordinated cell migration in crypts are clearly correlated with the functioning of the Eph/ephrins signaling pathway.[6] Because of the repulsive action of ephrins, those cells that express the ephrin ligand will sort away from those cells that are characterized by the presence of the Eph receptor and vice-versa. This would be the basic dynamical mechanism according to which a boundary between distinct cell population can be established (Kullander and Klein 2002). While proliferative, stem and Paneth cells mostly express EphB proteins, nondividing differentiated cells mainly express ephrinB proteins, because of the

[4] Erythropoietin-producing hepatoma-amplified sequence (Eph) receptors are transmembrane receptor tyrosine kinases (RTKs) and are grouped in two classes: A and B. They interact with cell surface ligands named ephrins, which are classified in two classes as well: Ephrins-A (tethered to the membrane through a glycosyl phosphatydyl inositol moiety) and Ephrins-B (which spans the membrane and are characterized by a short cytoplasmic tail). The most important property is that both ligands and receptors can give rise to a transduction-signaling cascade: Eph-activated signaling is forward, while ephrin-activated is backward.

[5] In detail, Eph/ephrins signaling is supposed to regulate several molecules involved in the adhesion processes, such as: integrins, fundamental in cell-extracellular matrix binding (Zou et al. 1999; Miao et al. 2000, 2005; Deroanne et al. 2003; Bourgin et al. 2007); cadherins, which mediate cell–cell contact adhesion (Tepass et al. 2002); connexins, which are the main structural units of gap junction communication (GJC) (Laird 1996); claudins which are components of specific junctions that restrict movements of molecules across the epithelial barrier (Hartsock and Nelson 2007).

[6] In small intestine there is a high concentration of A- and B- class Eph receptors, being the most abundant EphA1, EphB2, ephrinA1, ephrinB1 and ephrinB2 (Hafner et al. 2005). Beta-catenin (involved in Wnt signaling) and T cell factor (TCF) are supposed to regulate the positioning and the migration of epithelium cells in the crypts by means of the Eph/ephrin signaling pathway: Beta-catenin and TCF up-regulate EphB receptors and down-regulate their ligand ephrinB. It is found that the expression of EphB2 is higher at the bottom of the crypt, since Beta-catenin/TCF complex is involved in regulative transcriptional activities in the nuclei. Conversely ephrinB1 and ephrinB2 level is higher at the top of the crypt (Batlle et al. 2002; Holmberg et al. 2006).

activity of the signaling network. As a consequence, in a normal intestine Paneth and dividing cells are confined to the lower portion of the crypt (Batlle et al. 2002; Alberts et al. 2007).

The influence of Wnt signaling on the expression of EphB receptors recalls the complexity of the interplay between signaling pathways that characterizes the crypt dynamics.

Among the various other pathways entailed in crypt dynamics and homeostasis we only mention (for the lack of space): Hedgehog, bone morphogenetic proteins (BMP), Par polarity, and platelet-derived growth factor pathways. Besides, recent interest has been devoted to the interaction between stem cells and sub-epithelial myofibroblasts and other mesenchymal cells in the adult intestine (Gregorieff et al. 2005; Yen and Wright 2006; Brown et al. 2007; Kosinski et al. 2007; Lin et al. 2008; Samuel et al. 2009).

A picture of the crypt morphology and dynamics, as well as of the main signaling pathways involved in its homeostasis is provided in Fig. 1.

2.4 The colorectal cancer

The colorectal cancer (CRC) is one of the most diffused cancers worldwide and one of the major causes of death in adults (see e.g. Jemal et al. 2010). Most of the colorectal cancers develop through a number of morphological stages and their development is strongly correlated with the malfunctioning of the complex signaling network that rules the crypt dynamics and homeostasis (Fearon and Volgestein 1990; Kinzler and Vogelstein 2002; Frank 2007; Jass 2007; Medema and Vermulen 2011).

It is possible to distinguish different types of colorectal cancer according to the specific molecular and morphological features (Jass 2007 and further references therein):

- Standard progression (about 57 % of the total): it can be sporadic, Familial Adenomatous Polyposis (FAP)-associated (Galiatsatos and Foulkes 2006) or MUTYH-polyposis associated (Koinuma et al. 2004). It is usually associated to chromosomal instability and originates in adenomas (see Sect. 2.4.1).
- Hereditary nonpolyposis colorectal cancer (HNPCC) (3 %): it origins in adenomas and is characterized by mutations in B-RAF gene, in the mismatch repair (MMR) system (Boland 2002) and by Microsatellite Instability (MSI) (Thibodeau et al. 1993; Oki et al. 1999) (see Sect. 2.4.2).
- Hypermethylation-induced CRCs (40 %): it originates either in serrated polyps or in adenomas and is characterized by the aberrant methylation of promoter region CpG island (see Sect. 2.4.3).

2.4.1 Standard progression

We can briefly schematize the standard adenoma–carcinoma progression as follows (see Fig. 2).

First, one or more crypts manifest an accumulation of cells at their surface, which can form either hyperplastic or dysplastic tissues. Successively, polyps begin to grow

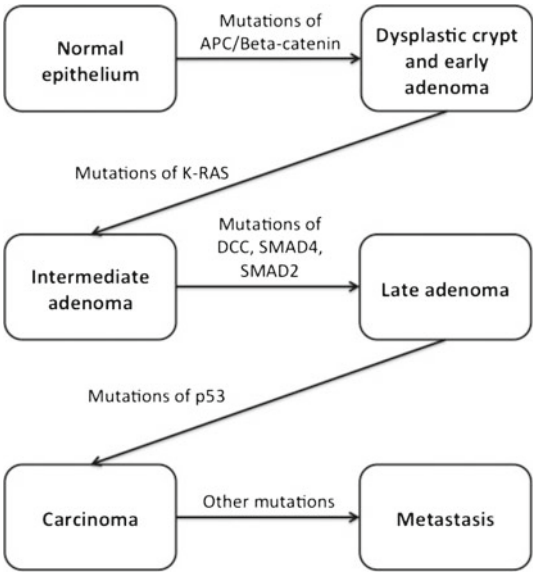

Fig. 2 Schematic representation of the standard progression of CRC (Frank 2007) (color figure online)

and project from the surface and, in case the polyps are dysplastic, these small precancerous tumors are defined *adenomas*, which are the preliminary potential manifestation of cancer (in a 30:1 ratio of adenomas to carcinomas Frank 2007).

One of the first recognized causes of the emergence of adenomas is the mutation of the tumor suppressor APC gene (found in 80 % of all colorectal adenomas and carcinomas Goss and Groden 2000), which is involved in the Wnt signaling pathway (see above) and negatively regulates the activity of the cytoplasmic levels of Beta-catenin (Munemitsu et al. 1995; Rubinfeld et al. 1997; Bienz and Clevers 2000; Sancho et al. 2004). Given that Beta-catenin enhances the expression of c-Myc and other proteins that favor cellular division, plays a role in adhesion processes (through surface receptors EphB2 and EphB3 Batlle et al. 2002) and is involved in the apoptosis control, the mutations of APC pathway, which releases Beta-catenin from its repressive effects, allow a possible aberrant expansion of the tissue (Fearon and Volgestein 1990; Kinzler and Vogelstein 2002).

It is hypothesized that the modification of APC pathway is the initiating event of colorectal cancer, because mutations in other genes are observed only in later stages of the progression or in non-malignant ones (e.g. non-malignant aberrant crypts usually display only mutations in K-RAS Nucci et al. 1997).[7]

Subsequent mutations of tumor suppressor RAS genes (usually in K-RAS but occasionally in H-RAS and N-RAS), which control a number of molecules involved in

[7] We remark that germline mutations in the APC gene are proven to be the cause of the inherited Familial Adenomatous Polyposis (FAP) syndrome, in which numerous adenomas develop during the third to the fourth decade of life. In presence of this syndrome the lifetime risk of CRC reaches nearly 100 % (Goss and Groden 2000).

GDP/GTP switches, and the mutational activation of specific oncogenes are correlated with next phases of the tumor progression (Kinzler and Vogelstein 2002).

The inactivating mutation of the TGF-Beta signaling pathway (e.g. SMAD-4 or TGFBR2) usually leads to a late stage of the adenoma (notice that it is hypothesized that mutations in genes DCC and SMAD2 play a role as well at this stage). Malignancy is then reached through the inactivation of the p53 gene in most of the cases (Kinzler and Vogelstein 2002), considered that p53 controls cell division and induces apoptosis in response to stress.

Alterations in the Eph/Ephrin bidirectional signaling are often correlated to disease and cancer (Pasquale 2005) and, in particular, the presence of EphA2, EphB and E-cadherin is strongly correlated with the progression of colorectal carcinoma (Saito et al. 2004). In this regard the loss of EphB genes would be correlated with the appearance of the invasive expanding of tumor cells. Moreover, there are evidences that Eph receptors may be converted into pro-oncogenetic proteins: it is hypothesized that cancerous cells avoid the anti-migratory effects of activated Eph receptors or even favor the migration and invasion triggering a signaling channel with oncogenetic partners (Wang 2011).

Most of colorectal cancers (85 %) display also chromosomal aberrations; the loss of heterozygosity (LOH) is supposed to hasten the genetic changes that drive carcinogenesis (Nowak et al. 2002b), as well as chromosomal instability (CIN), which arises from mutations and other genomic changes (Rajagopalan et al. 2003).

2.4.2 Hereditary nonpolyposis colorectal cancer, HNPCC

A significant percentage of colorectal cancers do not show CIN or chromosomal defects, while they conversely display mutations in the mismatch repair (MMR) system (Boland 2002), which are usually defined as Microsatellite Instability (MSI) (Thibodeau et al. 1993; Oki et al. 1999).

This is one of the causes of the so-called hereditary nonpolyposis colorectal cancer (HNPCC).[8] The morphological progression is similar to the standard one, but with differences in mutations and rates of progression and patients present an adenoma to carcinoma ratio of about 1:1 (Jass et al. 2002a,b).

We remark that HNPCC are characterized by a series of later mutations that are other than the classical pathways (Jass et al. 2002b).

2.4.3 Hypermethylation-derived CRC

Some colorectal cancers accumulate modifications in gene expression through the aberrant methylation of promoter region CpG island, which can influence various regulatory processes (Toyota et al. 1999). In some cases the hypermethylation induces the silencing of MMR, thus causing the reduction of the apoptosis rate followed by an increase in the rate of somatic mutations (Jass et al. 2002a). As a consequence 95 % of the crypt foci are hyperplastic and serrated and the remaining ones are dysplastic and

[8] Notice that *Lynch syndrome*, a particular hereditary disorder that is highly correlated with the risk of development of colorectal and other cancers at an early age, is often used as synonym of HNPCC.

without serration. In this case there is lack of chromosomal instability. In some other cases, there is no MSI and it is supposed that hypermethylation knocks out different DNA repair genes (Jass et al. 2002a), which would lead to rapid evolution of dysplastic serrated adenomas to carcinomas.

2.4.4 Other features of CRC

Recent findings point to stem cells as the cells from which tumors originate: the mutation of APC in stem cells may drive them toward a mutated state, according to which they would remain confined at the bottom of the crypt, while fueling the growth of micro-adenomas, which in turn would grow to their macro-form in a few weeks (Barker et al. 2009).

There are several other signaling pathways involved in the CRC development and, for lack of space, we just cite a few of the most important: bone morphogenetic proteins (BMP) and the hedgehog signal transduction pathway (given that the correlated autocrine/paracrine activation seems to be essential for tumor growth).

3 List of the essential phenomena in intestinal crypts

Here, we report a schematic list of the main phenomena which occur in the intestinal colonic crypts and which are object of the computational and mathematical modeling.

Normal tissue (Wong 2004; Crosnier et al. 2006 and further references therein)

- General major phenomena
  - General homeostasis.
  - Differential adhesion phenomena.
  - Apoptosis of differentiated cells (Adams and Cory 2007).[9]
  - Epithelial-mesenchyme interactions (Kedinger et al. 1986).
  - Immune surveillance.
- Cell positioning and movement (*dynamic turnover*)
  - Coordinate migration of cells in transit amplifying stage from the stem cell niche (in the lower part of the crypt) toward the top of the crypt (with the exception of Paneth cells, which move downward).
  - Cell sorting and hierarchical stratification.
  - Stem cell niche maintenance.
  - Dispersion of differentiated cells at the top of the crypts into the intestinal lumen.
- Cell differentiation processes
  - Presence of distinct lineage commitment fates

[9] Known to represent a barrier to cancer development.

  - Gradual differentiation of the stem cell progeny through transit amplifying stages, up to the completely differentiated stages, by means of several post-mitotic differentiation events.
  - Dynamics of clonal competition (Thirlwell et al. 2010).
- Intra- and inter-cellular pathways
  - Gene regulatory networks dynamics.
  - Signaling pathways dynamics (e.g. Wnt, Notch, Eph/ephrins, Hedgehog, PDGF,[10] BMP, etc.).
  - Intercellular communication and paracrine signaling.
  - Other metabolic pathways involved in the normal development and activity of the crypt.

Transformed tissue (Hanahan and Weinberg 2011 and further references therein).

- General major phenomena
  - Disruption of normal cell growth-and-division cycle and consequent interruption of general homeostasis.
  - Sustenance of chronic inflammation (Coussens and Werb 2002).
  - Avoidance of immune surveillance (Vajdic and Leeuwen 2009).
  - Disabling of apoptosis/senescence/autophagy mechanisms and activation of replicative immortality (through telomerase expression).
  - Disabling of contact inhibition mechanisms (which regulates proliferation).
- Aberrant cell types and modification in the differentiation process
  - Emergence of different tumor cell types.
  - Clonal heterogeneity (or polyclonality) (Thirlwell et al. 2010).
  - Presence of cancer stem cells (CSCs) (Reya et al. 2001).
- Mutations and alteration of pathways
  - Modification of various signaling pathways (Lemmon and Schlessinger 2010; Witsch et al. 2010 and references therein), such as: mitogenetic signaling, autocrine proliferative stimulation, negative feedback loops (e.g. Ras oncoprotein), ligand-receptor signaling (e.g. Notch, Neuropilin, Robo, Eph-A/B), TGF-Beta induced epithelial-to-mesenchyme transition (EMT) pathway (Ikushima and Miyazono 2010), etc.
  - Alterations in other key metabolic pathways, e.g. aerobic glycolysis, etc.
  - Genomic instability and genetic (somatic) mutations.
  - DNA hypermethylation or other epigenetic mutations.
- Interaction with other tissues and organs of the organism
  - Vascularization angiogenesis and related processes, such as: angiogenetic switch activation (Hanahan and Folkman 1996) and VEGF-A and TSP-1 mutations (Ras, Myc).
  - Invasion of the stroma and consequent interactions between the neoplastic and stromal cells within a tumor and the dynamic extracellular matrix that they shape (Egeblad et al. 2010).
  - Activation of invasion and metastasis (Talmadge and Fidler 2010).

[10] Platelet-Derived Growth Factors.

4 Classes of mathematical and computational models

The up-to-date computational models that can be used to describe the dynamics of intestinal crypt and the development of the colorectal cancer can be categorized into three broad categories:

- *Spatial models*: models that describe the spatial location of each individual cell; they can be further classified into two classes: in-lattice (or grid)-models and off-lattice (or lattice-free) models (see Sects. 5 and 6).
- *Compartmental models*: models that only describe the transition between cell types independently of their relative position in the crypt (Bjerknes 1996; Boman et al. 2001; Paulus et al. 1992).
- *Non-spatial stochastic models*: this category includes a wide range of models developed for specific purposes, such as the investigation of the consequences of APC hits, the analysis of the role of genetic instability or the prediction of colorectal cancer development starting from epidemiological data (Luebeck and Moolgavkar 2002; Nowak et al. 2002b; Komarova et al. 2003; Nowak et al. 2003; Komarova and Wodarz 2004; Komarova and Wang 2004; Wodarz and Komarova 2005; D'Onofrio and Tomlinson 2007; Di Garbo et al. 2010).

In this review, we will be focusing on the first category and we will describe in detail the following classes of models:

- *In-lattice* (or *grid*) models,
- *Off-lattice* (or *lattice-free*) models.

The description of each model will start with an in-depth analysis of its underlying mathematical computational features. Next, each model will be followed by a summary of its choice of *parameters*. Finally, we will describe how each model has been *validated* and against which biological data and process, always being wary of the"nature" of biological data and associated noise and of the particular goals of the research group that devised it.

5 In-lattice (or grid) models

The first lattice models of crypt dynamics characterized the crypt as a rigid 2D-grid (Loeffler et al. 1986, 1988; Paulus et al. 1993; Gerike et al. 1998; van Leeuwen et al. 2006). They relied upon a certain number of unphysical assumptions in order to simplify the representation and make the computation feasible. Basically, they were built under these simplifications: (a) the crypt is perfectly cylindrical in shape; (b) all cells occupy an equal rectangular area on the basal lamina, as they are uniformly arranged in pre-defined rows and columns; (c) migration takes place in cell-sized spatial steps; (d) the insertion of newborn cell causes a column of cells to shift upwards, breaking many cell–cell contacts; (e) cell motion is driven by mitotic pressure only: therefore migration stops only if cell proliferation is inhibited. The cylindrical crypt is opened and rolled out and mapped onto a rectangular grid through periodic boundary conditions. Each cell is labeled by its position on the grid and several other parameters. At discrete

time steps, cells are supposed to move between predefined rows and columns on the surface. When new cells are inserted into the grid according to pre-defined rules, a cell displacement occurs.

The main problem with this kind of approach is that the insertion of each newborn cell causes a whole column of cells to shift upwards, thus breaking many cell–cell contacts. This is unrealistic as epithelial cells are known to be linked by tight cell–cell junctions, forming a continuous network that prevents the lumen contents from entering the body.

5.1 The Glazier–Graner–Hogeweg (GGH) or cellular Potts method (CPM) model

More realistic assumptions are, instead, at the basis of the models built upon the well-known Glazier–Graner model (Graner and Glazier 1992, 1993) which, in turn, is based on Potts statistical mechanics ferromagnetic spin model. Among these derived models, the most important one is the so-called *Glazier–Graner–Hogeweg Model* (GGH).

The GGH model, also known as the *Cellular Potts Model* (CPM), is a mesoscopic model for simulating cell and tissue dynamics, keeping individual cell identity. Glazier and Graner first introduced the CPM to model and simulate cell re-arrangement by differential adhesion driven by cell adhesion molecules and they succeeded in reproducing cell sorting experiments. Here we briefly introduce the basic ideas underlying this model, with particular regard to its application to the modeling of intestinal crypts (following subsection).

The central input in the GGH model is the so-called *effective energy*, H,[11] which is the Hamiltonian of the system, and which rules the behavior of the cells and the interactions among them. The Hamiltonian includes the interactions between cells and other cells and the *extracellular matrix* (ECM) and some constraints that determine individual cell behaviors. The CPM was originally designed as a cell sorting model in two-dimensional aggregates (Graner and Glazier 1992, 1993). The main idea was to simulate cell re-arrangement using an extension of the two-dimensional Potts model which allows for constraints in cell size and for different surface energies between different cell types.

A collection of N cells is described by defining N degenerate spins $\sigma(i, j) = 1, \ldots, N$, where (i, j) label a lattice site. A cell σ consists of all sites in the lattice sharing the same value of spin. Cells form therefore domains (not necessarily simply connected and, if so, not necessarily convex) on a two-dimensional lattice. Each spin interacts with its nearest neighbors on a(n) (usually) square lattice. The corresponding interaction energy (or Hamiltonian) takes the form

$$H_{Potts} = \sum_{(i,j),(i',j')\text{neighbors}} \left[1 - \delta_{\sigma(i,j),\sigma(i',j')}\right], \tag{1}$$

where $\delta_{m,n}$ is the Kronecker symbol. Clearly, according to (1), two interacting spins want to line up in order to minimize the pair interaction energy: mismatched cou-

[11] H is eventually accompanied by a subscript that is related to the involved interaction.

plings between different cells have energy 1 and couplings between alike spins have energy 0. The evolution of the domains representing individual cells include protrusions and retractions and it follows a *Metropolis dynamics*: at each step a lattice site is selected at random and its spin is changed from σ to σ' with Monte Carlo probability

$$P\left(\sigma\left(i,j\right)\rightarrow\sigma'\left(i,j\right)\right)=\min\left\{1,\exp\left(-\frac{\Delta H}{kT}\right)\right\} \tag{2}$$

for $kT>0$, and

$$P\left(\sigma\left(i,j\right)\rightarrow\sigma'\left(i,j\right)\right)=\begin{cases}0 & \text{if} \quad \Delta H>0\\ \frac{1}{2} & \text{if} \quad \Delta H=0\\ 1 & \text{if} \quad \Delta H<0\end{cases} \tag{3}$$

for $kT=0$. Here T is the absolute temperature and k the Boltzmann constant. The factor kT gives account of the amplitude of the cell membrane (boundary) fluctuations.[12] ΔH is the energy gain produced by the change. This energy driving mechanism needs be supplied with additional components when the biological behavior has to be taken into account properly.

First, biological cells have a generally fixed range of sizes, thus imposing a constraint on their spatial evolution. To this end, an elastic area constraint is added, representing the tendency of a cell to reach its fixed target size, given the possible variations in the current size as a consequence of the overall dynamics. Moreover, differences in contact energies between cells of different types influence the cell motion and re-organization (on the basis of the so-called differential adhesion hypothesis, (DAH) Steinberg 1962) and, thus, an additional cell label, the *type* τ, is introduced.

The above energy H_{Potts} (1) turns into:

$$\begin{aligned}H_{sort}=&\sum_{(i,j),(i',j')\text{neighbors}}J\left(\tau\left(\sigma\left(i,j\right)\right),\tau\left(\sigma\left(i',j'\right)\right)\right)\left[1-\delta_{\sigma(i,j),\sigma(i',j')}\right]\\&+\lambda\sum_{\text{spin types }\sigma}\left[a\left(\sigma\right)-A_{\tau(\sigma)}\right]^2\theta(A_{\tau(\sigma)}),\end{aligned} \tag{4}$$

where $\tau(\sigma)$ is the type associated with the cell σ, $J(\tau,\tau')$ is the surface energy between spins of type τ and τ'; λ is the strength of size constraint [the lower the value, the easier it is to deform the cell's membrane (boundary)], $a(\sigma)$ the current area of the cell σ (dynamically evolving), and $A_{\tau(\sigma)}$ the target area for cells of type τ. The area constraint penalizes the increase of the area and, at the same time, the surface energy wants each cell to contain slightly fewer than $A_{\tau(\sigma)}$ lattice sites. Biological aggregates are also surrounded by a *hosting* fluid (ECM) which is usually marked with type $\tau=\mathrm{M}$: at variance with the other cells, the medium has unconstrained area. Therefore, the medium target area A_{M} is set to be negative and the corresponding area constraint is suppressed by including the Heaviside function $\theta(x)=\{0:x<0;1:x>0\}$ in (4).

[12] Above a critical fluctuation energy kT_c cell dissociate, below this critical value spins coalesce into compact cells.

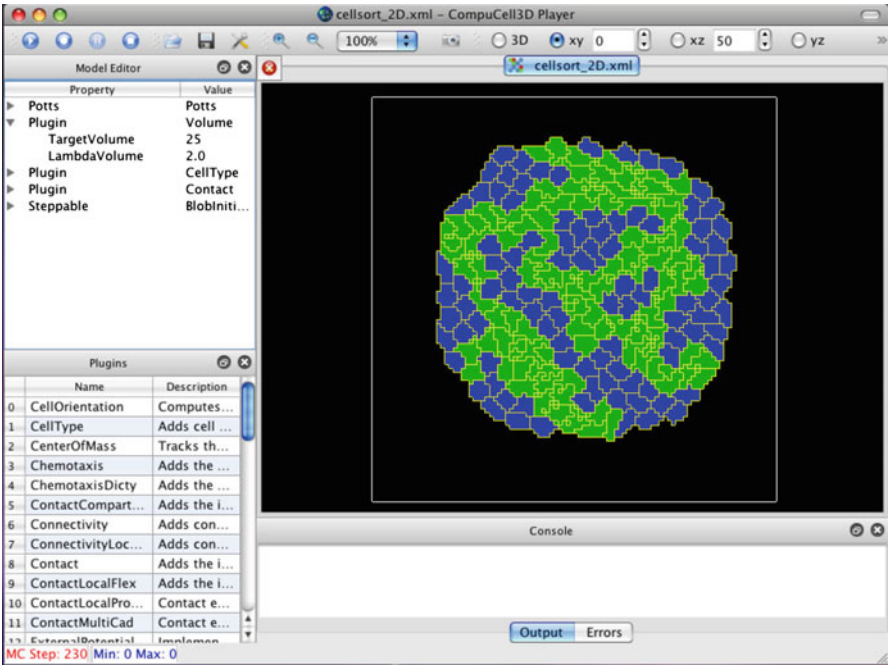

Fig. 3 Screenshot of a typical CompuCell3D simulation (http://www.compucell3d.org)

We remark that, given the properties of CPM, cell boundaries can crumple and diffuse, and that there are fluctuations in local contact angles, as well as lattice anisotropy, which can cause boundary pinning. Finite temperatures reduce the pinning, but implicate thermal fluctuations in contact angles and boundary shapes. Besides, the model does not distinguish among simply connected and multiply connected cells. At zero temperature, if cells are simply connected in the initial condition, multiply connected cells never occur, while at nonzero temperature surface fluctuations can create multiply connected cells, irregular cell shapes and detached cell fragments (as one can see in Figs. 3 and 4). In particular, cell boundaries can crumple if the temperature is comparable to the boundary energy.

Since the dispersal and crumpling is a biologically unrealistic artifact of the model, GGH make use of the annealing rule (i.e. $kT = 0$) of equation (3) by performing a certain number of zero temperature annealing steps, after the simulation at nonzero temperature.[13] Annealing allows the lattice configuration to re-equilibrate, gradually eliminating the crumpling effect on cell boundaries. Usually, in fact, after a simulation at nonzero temperature there are many crumpled boundaries, with numerous nearby

[13] GGH decide not to impose the nucleation of isolated heterotypic spins, to avoid the introduction of a biologically unrealistic constraint, considered that biological cells moving via the extension of lamellipodia usually implicates the loss of small tissue fragments and that the necking off of cell segments is common during mitosis. However, in this way the possible appearance of multiple connected cells is not prevented.

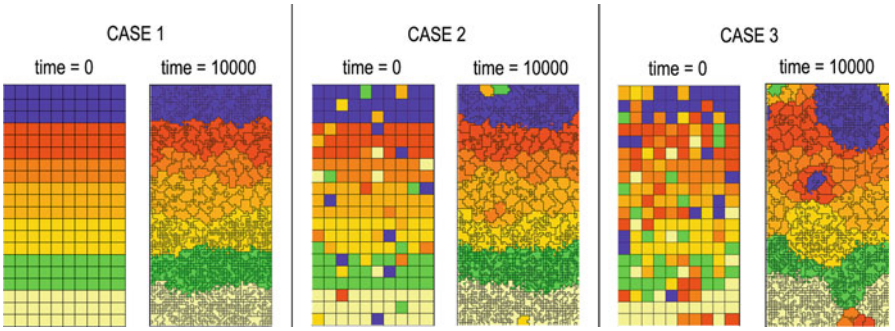

Fig. 4 Comparison between the outcome of three different simulations regarding an experiment of cell sorting in a crypt, using CompuCell3D. The crypts are represented on a 50×100 cellular automaton with periodic boundary condition on the x axis; the temperature is set to 30°, the neighborhood order is equal to 5. Cells are square-shaped and initially composed by 25 lattice sites. As in Wong et al. (2010) there are 7 cell types, Paneth cells (*yellow*, 30 cells in the initial conditions in case 1), stem cells (*green*, 30 cells), cells in transit amplifying stage 1 (TA1, *light orange*, 30 cells), TA2 (*orange*, 30 cells), TA3 (*dark orange*, 20 cells), TA4 (*red*, 30 cells) and differentiated cells (*blue*, 30 cells). The contact energy is set as in Wong et al. (2010) and the target area A_τ is set to 50 with λ in Eq. (4) equal to 2. No mitosis or differentiation processes are simulated. In case 1, all the cells are sorted according to their actual position in the crypt (see Sect. 2). The *left* figure represents the initial condition, while the *right figure* represents the state of the crypt after 10000 Monte Carlo steps (MCS). In case 2, 20 % of the cells in the initial conditions are randomly assigned among the 7 cell types. Also in this case, the two figures represent the state of the system at time 0 and at time 1000. In case 3, 40 % of the cells in the initial conditions are randomly assigned (color figure online)

disconnected regions composed by a few spins. A few annealing steps[14] makes most of the defects disappear.

The actual values of the external parameters in (4), i. e. $J(\tau, \tau')$, λ, A_τ, depend on the biology of the system. For instance (see also below) the coupling constants J are related to the adhesion and cohesion of cells which, in turn, depend on the receptor-ligand concentration on the cell membrane. In this sense, the internal genetic machinery of the cell determines the parameters entering the energy contributions in (4) so that the cellular genetic regulation is implemented via phenomenological parameters. On the other hand, these parameters are not accessible experimentally and this is one of the criticisms usually addressed to CPM. Nevertheless, the CPM model has been fruitfully employed to describe cell-sorting, cell positioning, re-arrangement and cell migration in aggregates (Graner and Glazier 1992, 1993). More complex biological phenomena, such as the development of the early stages of an embryo (i.e. *blastulation*) and the mitosis have been introduced in Mombach et al. (1993).

Notice that the model can be easily extended to the three-dimensional case in a straightforward way. Thus, in the general case the effective energy reads as

$$H_{sort} = \sum_{\boldsymbol{x},\boldsymbol{x}'\text{neighbors}} J(\tau(\sigma(\boldsymbol{x})), \tau(\sigma(\boldsymbol{x}')))[1 - \delta_{\sigma(\boldsymbol{x}),\sigma(\boldsymbol{x}')}]$$

[14] Given that annealing removes defects, but also evolves the patterns, only a certain number of steps is reasonable not to introduce possible biases in the simulation.

$$+\lambda \sum_{\text{spin types } \sigma} [a(\sigma) - A_{\tau(\sigma)}]^2 \theta(A_{\tau(\sigma)})$$
$$+\lambda' \sum_{\text{spin types } \sigma} [v(\sigma) - V_{\tau(\sigma)}]^2 \theta(V_{\tau(\sigma)}), \tag{5}$$

where the 3-dimensional vector $\boldsymbol{x}$ stands for a lattice site: in the simplest case of a simple cubic lattice $\mathbb{Z}^3$, $\boldsymbol{x}$ is a triplet of integers labeling a site where a spin is sited. $A_{\tau(\sigma)}$ now represents the surface (membrane) of the cell occupying the volume $V_{\tau(\sigma)}$: correspondingly λ is the resistance to membrane stretching and λ' the resistance to compression, $A_{\tau(\sigma)}$ and $a(\sigma)$ the target and current membrane areas, $V_{\tau(\sigma)}$ and $v(\sigma)$ the target and current cell volumes.

The corresponding transition probability is taken to be

$$P\left(\sigma\left(\boldsymbol{x}\right) \to \sigma'\left(\boldsymbol{x}\right)\right) = \left\{ \begin{array}{ll} \exp\left(-\frac{\Delta H + H_0}{kT}\right) & \text{if} \quad \Delta H > -H_0 \\ 1 & \text{if} \quad \Delta H < -H_0 \end{array} \right\}$$
$$= \min\left\{1, \exp\left(-\frac{\Delta H + H_0}{kT}\right)\right\} \tag{6}$$

where $H_0 \geq 0$ is an energy threshold which models viscous dissipation and energy loss during bond breakage and formation (Merks and Glazier 2005; Hogeweg 2000).

It is important to remark that CPM has shown to be rather versatile in describing patterning in biological tissues (Savill and Sherratt 2003), cancer cell metastasis (Turner and Sherratt 2002), and vasculogenesis (Merks et al. 2006). In the following, we describe the applications of CPM to colonic crypts.

Parameters setting and validation

The simulations concerning the variation of the configuration of the lattice were successfully compared with experiments on the formation of cell patterns during the sexual maturation of avian oviduct (Honda et al. 1986) and with experiments regarding the slug phase of the slime mold *Dictyostelium discoideum* (Takeuchi et al. 1988; Takeuchi and Tasaka 1989). The other main results were validated through the comparison with the experiments in (Honda et al. 1986) (cell patterning), (Steimberg and Garrod 1975; Nicol and Garrod 1979, 1982; Technau and Holstein 1992) (cell sorting), Gierer et al. (1972) (incomplete bulk sorting), (Jouanneau et al. 1992) (cell rigidity), (Armstrong 1989; Thomas and Yancey 1988) (engulfment and adhesion hyphotesis), (Armstrong and Parenti 1972; McClay and Ettensohn 1987) (incomplete sorting).

5.2 The Wong model: the application of CPM to intestinal crypts modeling

Recently, Wong et al. (2010), applied the CPM to the cell sorting and re-arrangement problem in the intestinal crypt epithelium.

Wong et al. (2010) have shown that differential adhesion between epithelial cells, triggered by the differential activation of EphB receptors and ephrinB ligands

(see Sect. 2) along is necessary in order to regulate cell positioning. Their model couples EphB/ephrinB interaction with crypt cell dynamics via CPM. EphB/ephrinB interaction is assumed to regulate the cell adhesion parameters $J(\tau, \tau')$ within the CPM effective energy H_{sort} [(4) and (5)]. Previous studies (Graner and Glazier 1992, 1993; Turner and Sherratt 2002) showed that differential adhesion alone is sufficient to govern cell re-arrangement and cell sorting. When cells of different adhesive properties are mixed together, cells with weaker binding tend to be displaced/driven by those with stronger adhesiveness. For instance, if two types of cells are mixed and one has stronger binding than the other, then the cells with stronger adhesion will cluster at the center of the aggregate, while the cells with weaker adhesion will remain at the periphery of the aggregate.

Here we briefly review the results has been obtained in Wong et al. (2010). Wong et al. used a 2D lattice model of CPM type to describe the dynamics of the crypt cells. More specifically, they represented the crypt as a cylindrical surface rolled out onto a plane with imposed periodic boundary conditions, thus ending up with a 2D rectangular lattice. They used the effective energy (4) and they assumed that cells belong to seven different types: Paneth cell (P), stem cell (S), four generations of transit-amplifying cells (TA1, TA2, TA3, TA4) and differentiated post-mitotic cell (D). The corresponding matrix of coupling constants $J(\tau, \tau')$ is provided in Fig. 2 of Wong et al. (2010).

Wong et al. considered cell growth and division in their simulation study. At division, every cell splits into two cells: a stem cell divides into another stem cell and into a TA1, a TA1 cell divides into two TA2 and so on, a TA4 cell divides into two D cells.

The division dynamics occurs as follows: after a predefined time lapse the target area is automatically doubled; accordingly, because of the elastic area constraint in the effective energy H_{sort} (4), the current area adapts to the new target quasi-instantaneously and the cell splits in two new cells. One of the two cells keeps the type of the progenitor, the other one changes identity according to the supposed lineage specification. Once that a specific cell reaches the top of the lattice, because of the mitotic pressure, it is expelled from the system and this is the way how the dynamic turnover is accomplished in the model.

In order to keep stem cells at their original initial positions, Wong et al. added an anchoring energy to the CPM hamiltonian (4)

$$H_S = \sum_{(i,j)} J_{\text{niche}} \left(1 - \delta_{M_{ij},\tau(\sigma(i,j))}\right) \tag{7}$$

where J_{niche} is the adhesion energy (anchoring) between the cell and the initial stem cell position, recorded in M_{ij}.[15] The entries of the coupling matrix $J(\tau, \tau')$ are supposed to be strictly connected with the spatial gradients of proteins present in the intestinal crypt (i.e. EphB and ephrinB), as the location of a cell in the crypt is related to its differentiation stage and hence to the type. Notice that the gradients are supposed to be assigned, i.e. EphB2 expression decreases towards the top, while ephrinB1 and ephrinB2 ones decrease towards the bottom of the crypt (Fig. 1). In particular, a high level of EphB receptor activation by ephrinB reduces cell adhesion and vice-versa.

[15] If (i, j) corresponds to a stem cell, that is $\tau(\sigma(i, j)) = \text{S}$, then $M_{ij} = \text{S}$.

As the expression of ephrinB increases and that of EphB decreases from the bottom to the top, differentiated cells at the upper part of the crypt have a high concentration of ephrinB and the lowest expression of EphB and accordingly $J(\mathrm{S,D}) > J(\mathrm{S,TA4}) > \cdots > J(\mathrm{S,P}) > J(\mathrm{S,S})$, and so on for the other entries of $J(\tau, \tau')$.

All the assumptions above about the model that Wong et al. have set in their computation are meant to reproduce appropriately the correct cell positioning and sorting as observed experimentally in the crypt. They also performed studies of the sensitivity upon varying the surface energies $J(\tau, \tau')$ and they found a certain general robustness. They concluded that, according to their model, differential adhesion regulates positioning of cells. Moreover, they found that cells migrate vertically towards the top of the crypt and this motion is coordinated, leading to the maintenance of the homeostasis of the entire crypt system.

Nevertheless, we must point out that, in general, spatial patterns can derive as a consequence of reaction and diffusion processes taking place among cells and concerning the exchange of nutrients and other signals (see, e.g., Greenberg et al. 1978; Bunow et al. 1980; Koga and Kuramoto 1980; Othmer and Pate 1980; Grindrod 1991). In a way, the cell arrangement is also the result of an equilibrium in reaction and diffusion mechanisms and the assumption on the gradients of proteins should actually be an outcome of this overall equilibrium. For example, chemotaxis can be incorporated in CPM model to investigate the role of chemoattractant concentration in directional cell sorting.

Parameters setting and validation

The distribution of stem cell is based on the scenarios proposed in Potten et al. (1997) and Barker et al. (2007), while the adhesion energy matrix is based on the experimental results in Poliakov et al. (2004) and in those mentioned in Wilkinson (2003) and further references therein.

The results on cell migration and cell patterning were verified with the comparison with the *in vivo* experiments presented in Winton et al. (1988) and with the experimental studies in Batlle et al. (2002) and Clevers and Battle (2006), the re-distribution of proliferative cells was compared with the observations in Holmberg et al. (2006), the speed of the directed migration in simulations was confirmed through the comparison with the experiments in Tsubouchi (1983), the coordinated migration was compared to the results in Haga et al. (2005), while the results concerning cell homeostasis were proven to be consistent with experimental observations in Meineke et al. (2001).

A digression on stem cell dynamical organization

It is worth noticing that in Wong's simulation study, cell division is symmetric, i.e. daughter cells have the same identity, for all cell type but the stem cells. For these latter the division is actually assumed to be asymmetric and it leads to a stem cell and a TA1 cell. Intrinsic division asymmetry is actually the most popular view on how stem cell populations accomplish homeostasis. Such an assumption falls within the so-called *hierarchical* models. Alternative assumptions are available in literature and are the subject of intense research activity which points at studying the stem cell organization

and dynamics in small intestine and colon. Actually, recent studies (Snippert et al. 2010) have shown that most stem (Lgr5) cell divisions occur symmetrically and do not support a model in which two daughter cells resulting from a stem cell division adopt divergent fates. The corresponding cellular dynamics has been shown (Lopez-Garcia et al. 2010) to be consistent with a model in which the basal stem cells double their number each day and stochastically follow stem or TA fates. Accordingly, cell fate is determined by competition for available niche space at the crypt base so that homeostatic stem cell maintenance is guaranteed by a neutral competition between equal stem cells occurring at the population level and not at the level of a single cell. In the stem cell population, cell loss is compensated by the multiplication of a neighboring cell, leading to a *neutral drift dynamics* in which clones expand and contract randomly, until they migrate upwards in the crypt and keep differentiating or migrate downward and become Paneth cells. The rate of stem cell replacement is comparable to the cell division time, thus entailing that drift and symmetrical division are fundamental for stem cell homeostasis. The chance of finding a persisting clone with a size larger than n stem cells at a time t obeys a scaling relation

$$P_n(t) = f\left(\frac{n}{\langle n(t)\rangle}\right), \tag{8}$$

where $f(.)$ is a characteristic scaling function and $\langle n(t)\rangle$ denotes the average clone size. Calculations have shown that $f(x) = \exp\left(-\frac{\pi x^2}{4}\right)$ (Lopez-Garcia et al. 2010). The scaling behaviour entails that stem cells form a single functionally equivalent group and the entire drift dynamics tends to monoclonality. On the experimental side, the migration streams of intestinal cells on the close villi have been used to analyze indirectly the dynamics of the underlying stem cell compartments. On the mathematical side, theoretical predictions are made on the basis of a one-dimensional coalescing random walk (Lopez-Garcia et al. 2010). Moreover, recent additional studies (Sato et al. 2011) suggest that Paneth cells may function as niche-supporting cells. After symmetrical division, stem cells undergo neutral competition for contact with Paneth cells surface. When detached, cells loose access to short-range signals that maintain their stemness and start migrating and differentiating along the crypt axis.

Notice that other distinct hypotheses on stem cell properties and organization have been recently proposed and corroborated by an increasing number of experimental evidences.

In particular, according to Roeder, Loeffler and others (Roeder and Loeffler 2002; Glauche et al. 2007; Roeder et al. 2007), it is possible to understand stem cell organization (in particular, of hematopoietic stem cells) without specific assumptions on unidirectional developmental hierarchies, preprogrammed asymmetric division events or particular assumptions regarding a predetermined stem cell entity. The idea is to interpret stem cells as *nonhierarchical self-organizing dynamical systems* and *"stemness"* not as an explicit cellular property, but as the result of a dynamical process depending on individual cell potential and microenvironmental influence. Basically, the properties of stem cells are considered to permanently fluctuate, with some cells sometimes encountering a process of clonal expansion. In this regard, stem cells would be selected and modified in response to cell–cell and cell–microenvironment

interactions on the basis of their potential and flexibility, rather than being specialized a priori. This hypothesis has proven effective in explaining various observed properties of stem cells, e.g., the capability to proliferate, differentiate and self-renew, the functional heterogeneity, the microenvironment dependency of stem cell quality, the reversibility of cellular properties, the self-organized regeneration after damage, the fluctuating activity and competition of stem cell clones, etc.

Also according to Zipori (2004) stem cells are characterized by highly promiscuous gene-expression patterns, hinting at stemness not as a specific entity, while rather as a state that can be assumed by any cell and related to the capacity to renew and to differentiate into many cell types. In this regard, there can be transitions between the stem and proliferative states and, even if the transition to differentiation reduces the potential to return to the other states, some differentiated cells might indeed revert to the stem state, suggesting important reversibility and flexibility features of cell fate decision processes.

Further developments. As discussed in Sect. 2.4, the importance of studying stem cell dynamical organization and its strict connection with the sorting dynamics of the crypt resides in the fundamental role that this aspect has for understanding carcinogenesis in colonic crypts (Barker et al. 2009). In light of the above, it is then reasonable to conceive a further improvement of Wong model in order to account for the homeostatic maintanence of stem cell compartment in the CPM lattice cell discretization and to put it inline with the homeostasis of the entire crypt system.

Besides, we remark that the interpretation of stem cells as self-organizing dynamical systems as that proposed by Roeder, Loeffler, Zipori and other is indeed consistent with that at the base of the multiscale model of intestinal crypt dynamics in phase of development (Graudenzi et al. 2012) and briefly introduced in the conclusions.

5.3 Other extensions of the CPM model

In real biological systems the overall dynamics and homeostasis are ruled by a complex interplay between intra- and inter-cellular processes, with particular regard to chemotaxis, signaling pathways, gene regulation, food availability, etc. In this regard, several developments of the CPM model have been designed in the course of time in order to provide a fine description of these specific mechanisms. We will cite a few of the most important.

5.3.1 Chemotaxis

Savill and Hogeweg (1997) provided a hybrid extension of the CPM in order to model *chemotaxis*. To this end, one needs to introduce the concentration *field* $c(\boldsymbol{x}, t)$ (t denotes the time) of the chemoattractant chemical, upon discretizing it over the CPM lattice. The dynamics of c is then defined by a set of ordinary differential equations (ODEs) describing the *internalization* dynamical processes of cell's secretion and absorption of the chemical, and a set of partial differential equations (PDEs) that describe the spatial diffusion and decay of the chemical, ignoring advection.

Accordingly, in order to make cells move preferentially up chemoattractant gradients, in Savill and Hogeweg (1997) the authors add a term in the CPM effective energy (5) ending up with a hamiltonian of the form

$$H' = H_{sort} - \mu \sum_{\boldsymbol{x},\boldsymbol{x}'} \frac{c(\boldsymbol{x},t)}{sc(\boldsymbol{x},t)+1}\left[1-\delta_{\sigma(\boldsymbol{x}),\sigma(\boldsymbol{x}')}\right], \tag{9}$$

where μ is a degree of chemotactic response of the cell: it can be either positive (chemoattractant) or negative (chemorepellent). The additional term comes from the standard Michaelis-Menten (1913) model and in Savill and Hogeweg (1997) s, a Michaelis-Menten constant, is taken to be vanishing, so that the change in energy for the Monte Carlo simulation would be

$$\Delta H' = \Delta H_{sort} - \mu \sum_{\boldsymbol{x},\boldsymbol{x}'} \Delta c(\boldsymbol{x},\boldsymbol{x}',t)\left[1-\delta_{\sigma(\boldsymbol{x}),\sigma(\boldsymbol{x}')}\right] \tag{10}$$

where $\Delta c(\boldsymbol{x},\boldsymbol{x}',t) = c(\boldsymbol{x},t) - c(\boldsymbol{x}',t)$ is the difference in the concentration of the chemoattractant between two neighboring sites of the lattice. When the sites $\boldsymbol{x}$ and $\boldsymbol{x}'$ belong to the same cell then the additional terms in (10) do not play any role in determining the gain or loss of effective energy and, in turn, the probability of transition (copying) of one site into the other. Otherwise, the change in energy (whether positive or negative) depends on the local difference in the concentration c and on the sign of μ. The cell's motion is biased up or down a field gradient by changing the calculated effective energy change used in the Monte Carlo probability (6).

In practice, the actual occurrence of transition depends on μ and Δc: if $\mu > 0$ and $c(\boldsymbol{x},t) > c(\boldsymbol{x}',t)$, then the change in energy due to the chemotaxis energy term (10) is negative, increasing the probability (6) of accepting the copy of the spin. The net effect is that the corresponding cell moves up the field c gradient with velocity $\mu\nabla c$. If $\mu < 0$, the cell will move down the field gradient. As for the values of the concentration field c over the lattice, these are determined by a reaction-diffusion-type partial differential equation of the form

$$\frac{\partial c(\boldsymbol{x},t)}{\partial t} = \operatorname{div}(D(\boldsymbol{x})\nabla c(\boldsymbol{x},t)) - k(\boldsymbol{x})c(\boldsymbol{x},t) + s(\boldsymbol{x}) \tag{11}$$

where $D(\boldsymbol{x})$, $k(\boldsymbol{x})$, $s(\boldsymbol{x})$ denote respectively the diffusion coefficient, the decay coefficient and the secretion rate. $D(\boldsymbol{x})$, $k(\boldsymbol{x})$, $s(\boldsymbol{x})$ may vary with position and cell-lattice configuration.

In more detail, in Savill and Hogeweg (1997) the authors studied the chemotaxis of the chemical attractant cAMP by using a simplified model based on Fitzhugh–Nagumo equations for the production, diffusion, secretion and absorption of the chemical.[16]

[16] Notice that the complex intracellular dynamics can be more accurately described by a more complicated system of ODEs, as proposed in Martiel and Goldbeter (1987) with a model based on the receptor desensitization for cAMP signaling, which is effective in accounting for experimentally observed phenomena, such as oscillations, excitability and adaptation.

As a result, in Savill and Hogeweg (1997) it was shown that the interplay among the production of cAMP, the chemotaxis to cAMP and the cellular adhesion processes causes the cells in a 3D lattice to spatially self-organize leading to the complex behavior of stream and mound formation, cell sorting and slug migration all without any change of parameters during the complete morphogenetic process.

Parameters setting and validation

The setting of the simulations is based on cell fate and cell differentiation hypotheses (Wang and Schaap 1989; Zimmerman and Weijer 1993).

The results on cell sorting were validated through the comparison with the experiments in Springer and Barondes (1978), Sternfeld (1979) and Sekimura and Kobuchi (1986), while the results on slug migration with the experiments in Siegert and Weijer (1992).

5.3.2 Further spatial constraints

In Hogeweg (2000) introduced *cell death by squeezing*: depending on the surface bond energies $J(\tau, \tau')$ and on the elasticity coefficients λ, λ', a cell may be reduced to zero volume, i.e. it may die. She also introduced *cell growth by stretching* and *volume-triggered cell division* (a mechanism which is similar to the one employed by Wong et al.): when the actual size of a cell $v(\sigma)$ exceeds the target size $V_{\tau(\sigma)}$ plus a threshold, the target volume is increased and when it has become twice the reference cell size the cell divides.

Parameters setting and validation

The rules for cell growth and divisions are based on experimental observations on stretch and squeeze in relation to cell growth and apoptosis (Chen 1997; Ruoslahti 1997).

5.3.3 Introducing gene regulatory networks

Hogeweg (2000, 2002) modelled cell differentiation by using the state of a Boolean network, a simple model of the genetic regulatory network, with inputs from neighboring cells, combined with a simple lock-and-key model of cell adhesion molecules in order to determine the bond-energies $J(\tau, \tau')$. She modeled in this way the role of cell adhesion molecules in inter-cellular signaling. The network served as a model of gene regulation, intercellular signaling and differentiation as well. Cell differentiation occurs through induction by neighboring cells.

The bond-energies can be modified, in real biotic systems, by peripheral processes, e.g. receptor clustering. Hogeweg's model of differentiation can also partly model peripheral processes even though her Boolean network is verbally meant to be a

gene-regulation network. As we have seen above for Wong et al.'s model of crypt dynamics, alternative methods for cell differentiation simply use prescheduled type (τ) changes of the cells.

5.3.4 Introducing signaling pathways

Savill and Sherratt (2003) incorporated in CPM a sub-cellular model of membrane-bound Delta–Notch signaling and combined it with a discrete-state differentiation model to explore the ability of several hypothetical scenarios to explain clustering and adhesion of stem cells. They use a system of simultaneous ODEs defined on the boundaries of stem cells with neighboring stem cells. In detail, these ODEs govern the evolution of the Delta expression on the boundaries of stem cells and the evolution of the bound Notch receptor (Delta–Notch complex) on the surface at each pixel. These equations account for several phenomena: (a) the background production rate of Delta in each cell, (b) the production rate of Delta induced by the level of Notch activation in each cell, (c) the reaction rate of Delta in each cell with free Notch on neighbouring cells, (d) the disassociation rate of the Delta–Notch complex, (e) the decay rate of Delta, (f) the reaction rate of Delta on neighbouring cells with free Notch in the cell, (g) the disassociation rate of the Delta–Notch complex and finally (h) the internalization rate of bound Notch.

Parameters setting and validation

The stem and transit-amplifying cell-cycle times, as well as the time that a committed cell resides in the basal layer are taken from experiments of human keratinocytes (Dover and Potten 1988).

The general rules for active cluster size control via regulation of differentiation have been (partially) validated by integrating the results on: over-expression of Delta–Notch (Lowell et al. 2000), average cell division time (Dover and Potten 1988), average time of irreversible commitment to differentiation (Adams and Watt 1989), adhesiveness properties (Jensen et al. 1999) and lateral-induction (Lewis 1998).

5.4 Shirinifard's model: a CPM-based model for tumor development

Many distinct processes, mechanisms and phenomena are essential for a possibly exhaustive and coherent description of multicellular systems as, for instance, chemotaxis or nutrients uptake. To this end, CPM reveals a certain degree of flexibility by allowing for the inclusion of multiple biological mechanisms and, accordingly, of multiple PDEs modeling them. Here, we limit ourselves to remark, as an example, that the hybrid model CPM-PDEs has been further extended recently to model three-dimensional multicellular systems including *vascular* tumor growth and angiogenesis in Shirinifard et al. (2009). To the best of our knowledge, no applications in this sense have been considered yet to crypt dynamics and colon rectal cancer.

Shirinifard et al.'s model consists of a 3D multicellular simulation of vascular tumor growth and it can be extended to describe more specific vascular tumor types and

hosting tissues (the extracellular matrix ECM in the terminology of CPM). The model contains *tumor* cells and *endothelial* cells (EC). These latter can be of two types: *vascular* and *neovascular*. All types are associated with different behaviors and properties. Moreover, three *fields* are included: *partial pressure of oxygen* $P(\boldsymbol{x}, t)$, *long-diffusing pro-angiogenic factor* VEGF-A $V(\boldsymbol{x}, t)$ and *short-diffusing chemoattractant* $c(\boldsymbol{x}, t)$. All these fields are discretized over the CPM grid.

The model contains three tumor-cell types: *normal, hypoxic, necrotic* and normal and hypoxic ones are referred to as tumor cells. Normal cells turn into hypoxic when the oxygen partial pressure $P(\boldsymbol{x}, t)$ is below a threshold value p_1 and they can turn into necrotic below a second threshold value $p_2 < p_1$. All the three types of tumor cells and both vascular and neovascular cells enter the GGH effective energy model (5) and they thus call for bond-energies $J(\tau, \tau')$ in order to make them interact with neighboring cells in the hosting tissue. Tumor cells are supposed to take up oxygen and proliferate according to a Michaelis-Menten-type law for the rate of the corresponding target volume

$$\frac{dV_{\text{tumor}}}{dt} = \frac{g P(\boldsymbol{x}_c, t)}{p_0 + P(\boldsymbol{x}_c, t)}, \tag{12}$$

where $\boldsymbol{x}_c$ is the center of mass of the tumor cell (obtained by using the site coordinates belonging to the cell), p_0 a prescribed constant and g is a growth rate constant (the previous assumptions being based on theoretical considerations only). As described above, the division of a cell occurs when the current volume doubles. Necrotic cells are supposed to disappear from the system according to a decay law

$$\frac{dV_{\text{necrotic}}}{dt} = -k_n < 0, \tag{13}$$

where V_{necrotic} is the target volume of necrotic cells.

In the model the pro-angiogenic factor VEGF-A is incorporated and described by the concentration field $V(\boldsymbol{x}, t)$. The dynamics of this field is described by a PDE of the form as in Eq. (11), i. e.:

$$\frac{\partial V(\boldsymbol{x}, t)}{\partial t} = -\varepsilon_V V(\boldsymbol{x}, t) + \delta(\tau(\sigma(\boldsymbol{x})), \text{hypoxic}) \alpha_V V(\boldsymbol{x}, t) + D_V \nabla^2 V(\boldsymbol{x}, t) \tag{14}$$

where now $\delta(\tau(\sigma(\boldsymbol{x})), \text{hypoxic}) = 1$ at the lattice sites belonging to hypoxic cells and it vanishes elsewhere, meaning that hypoxic cells secrete VEGF-A (at a constant normalized rate $\alpha_V = 1$), while over all the cells of the lattice VEGF-A diffuses with diffusion constant D_V and decays at a rate ε_V.[17] Hypoxic cells stops secreting VEGF-A factor and become normal whenever $P(\boldsymbol{x}, t) > p_1$ and become necrotic when $P(\boldsymbol{x}, t) < p_2$ when they start dying. The dynamics of $P(\boldsymbol{x}, t)$ is governed by a

[17] ∇^2 represents the laplacian operator.

PDE of the same type as in (14), i.e. it evolves as follows

$$\begin{aligned}\frac{\partial P(\boldsymbol{x},t)}{\partial t} = &-\min\left\{\varepsilon_0^{\text{tissue}} P(\boldsymbol{x},t),\, O_{max}^{\text{tissue}}\right\}\delta(\tau(\sigma(\boldsymbol{x})),\text{ECM})\\ &-\min\left\{\varepsilon_0^{\text{tumor}} P(\boldsymbol{x},t),\, O_{max}^{\text{tumor}}\right\}\delta(\tau(\sigma(\boldsymbol{x})),\text{tumor})\\ &+D_0\nabla^2 P(\boldsymbol{x},t).\end{aligned} \tag{15}$$

Here, $\varepsilon_0^{\text{tissue}}$ and $\varepsilon_0^{\text{tumor}}$ are, respectively, the oxygen consumption rate for the hosting tissue (ECM) and for both normal and hypoxic cells. O_{max}^{tissue} and O_{max}^{tumor} represent the maximum saturation rates for the tissue and the tumor cells, respectively; D_0 is a diffusion coefficient.

In turn, neovascular cells are categorized into subtypes: *inactive* and *active*. Vascular cells form a capillary-like network, i.e. the mature vasculature, whose integrity is maintained by an elastic energy of harmonic springs connecting their centers of mass: connectivity between neighboring vascular cells is lost when a threshold inter-distance is reached. Inactive neovascular cells have the same behavior as vascular ones with the additional property that above a threshold value V_0 of the VEGF-A field $V(\boldsymbol{x},t)$ they turn into active neovascular cells and start proliferating. Moreover contact-inhibited growth of neovascular cells is accounted for by stipulating that under a threshold contact area with other cells their target volume increases according to

$$\frac{dV_{\tau(\sigma)}}{dt} = \frac{G_v V(\boldsymbol{x}_c,t)}{nV_0 + V(\boldsymbol{x}_c,t)} \tag{16}$$

where $\tau(\sigma) =$ neovascular, n is a scaling constant and G_v the maximum growth rate. Active neovascular cells can chemotax up gradients of $V(\boldsymbol{x},t)$. The chemotaxis up to gradients of $V(\boldsymbol{x},t)$ is modelled by a Hogeweg term of the type in Eq. (9) with respect to the field $V(\boldsymbol{x},t)$ at the boundaries of active neovascular cells

$$\Delta H_{chemotaxis} = \left[\mu(\boldsymbol{x}) - \mu(\boldsymbol{x}')\right]\left[\frac{V(\boldsymbol{x},t)}{sV_0 + V(\boldsymbol{x},t)} - \frac{V(\boldsymbol{x}',t)}{sV_0 + V(\boldsymbol{x}',t)}\right], \tag{17}$$

and $\Delta H_{chemotaxis} = 0$ at the boundaries between two endothelial cells.

Equation (15) accounts for diffusion of oxygen over the system (CPM grid) and consumption of it in ECM and tumor cells. Vascular and neovascular cells consume and supply oxygen, acting as sources with constant oxygen pressure defined as follows

$$\begin{aligned}P_{\text{EC}}(\boldsymbol{x}) = &\; P_{\text{blood}}^{\text{vascular}}\delta\left(\tau\left(\sigma\left(\boldsymbol{x}\right)\right),\text{vascular}\right)\\ &+P_{\text{blood}}^{\text{neovascular}}\delta\left(\tau\left(\sigma\left(\boldsymbol{x}\right)\right),\text{neovascular}\right),\end{aligned} \tag{18}$$

where $P_{\text{blood}}^{\text{vascular}}$ is the oxygen partial pressure in the preexisting capillaries and $P_{\text{blood}}^{\text{neovascular}}$ is the oxygen partial pressure in tumor-induced vasculature.

Growth and chemotaxis of active neovascular cells up gradients of VEGF-A generate a dispersed growing population of neovascular cells rather than a capillary-like network pattern as for vascular cells. On the other hand, in order to favor

self-organization of endothelial cells (vascular and neovascular), the model also includes chemotaxis to a very short-diffusing chemoattractant represented by the field $c(\boldsymbol{x}, t)$. Accordingly, endothelial cells tend to self-organize themselves into capillary-like networks, thus pointing at preserving the preexisting structure. The corresponding PDE is a specialization of (11), i.e.

$$\frac{\partial c(\boldsymbol{x}, t)}{\partial t} = \alpha_c \delta(\tau(\sigma(\boldsymbol{x})), \mathrm{EC}) - \varepsilon_c c(\boldsymbol{x}, t)\,[1 - \delta(\tau(\sigma(\boldsymbol{x})), \mathrm{EC})] + D_c \nabla^2 c(\boldsymbol{x}, t), \tag{19}$$

where α_c is the secretion rate constant (effective for endothelial cells only), ε_c is a constant rate at which the chemoattractant degrades outside the domain of endothelial cells and D_c the constant rate at which the chemoattractant $c(\boldsymbol{x}, t)$ diffuses everywhere. Accordingly, an energy term is added to H_{sort} (5) of the same type as in (9).

The balance of all the above mechanisms dictates the dynamics of the system and describes the growth and the morphology (from spherical to cylindrical shape, to other possible shapes) of the vascular tumor domain around the vasculature network and possibly the breakdown (damage) of the network itself (see Shirinifard et al. 2009).

Parameters setting and validation

Some key parameters of the model were set on experimental data from (Burgess 1997; Fotos et al. 2006) (cell movement and speed), (Serini et al. 2003) (diffusion constants).

The observation regarding the growth of avascular tumors were compared with (Fischer et al. 2005) while other results were compared with distinct computational models (Zheng et al. 2005; Macklin et al. 2009).

Further developments

The above additional mechanisms are just some examples of implementation of a line of thought in mathematical and computational modeling that consists in "appending" several additional discretized fields to the basic CPM, thus extending its potentialities in applications. In this sense, Wong et al.'s model could be further extended to include nutrients' uptake (oxygen and glucose) in colonic crypt dynamics. This is work in progress and we plan to report about it in due course.

5.5 Computational tools based on the CPM: CompuCell3D

In Sect. 7, we will collect information about software and tools available for the various models object of this review. Here, we focus on one of them, related to CPM model.

There are several systems that implement the basic CPM with various extensions. Two of them are BioCellSim (Harrison 2010) and CompuCell3D (http://www.compucell3d.org). CompuCell3D is the software built by Glazier's group and is the one we used the most in our initial experimentation.

CompuCell3D is an open source tool that, as the website states, is mainly used to "study cellular behavior". The tool is presented as a partial differential equation solver, which is a description of the general capabilities of the Potts-model solvers.

CompuCell3D has a C++ core wrapped with Python scripting code in order to ease the process of writing extensions and plugins. As an example of its versatility, CompuCell3D has been recently tied to the `roadRunner` reaction simulation module of the Systems Biology Workbench (SBW) (cfr. the http://www.sys-bio.org site).

We used CompuCell3D for the simulation of a *de-novo* simplified model of crypt (i.e., we did not re-use the examples provided by the CompuCell3D distribution). To this end we based the main settings of the system on the data from Wong et al. (2010), with the basic goal of reproducing the cell sorting phenomenon. In particular, we simulated a cylindrical crypt on a 2D automaton with periodic boundary condition (on the x-axis), in which any (biological) cell is composed (in the initial condition) by a standard number of lattice sites and is characterized by a specific cell type. The dynamics is only due to the contact energies between different cell types (as taken from the energy contact matrix in Fig. 2 of Wong et al. 2010) and to an area constraint. No mitosis or differentiation processes are modeled in this case.

We performed three experiments and reported the outcome in Fig. 4. In the different experiments the crypts are characterized by distinct initial conditions for what concerns the position of the cells (the other features are common and fixed, see the caption of Fig. 4). In detail, in the first case (that is the control case) we positioned the cells as they are supposed to reside within real crypts, i.e. Paneth and stem cells in the lower bands, transit amplifying stage cells in the middle part and differentiated cells in the upper section. In the second (respectively third) experiment a random cell type is assigned to 20 % (respectively 40 %) of the cells (randomly chosen).

Looking at Fig. 4, we can observe that in the first case, as expected, the stratified positioning of the cell types is maintained in the course of the simulation (which lasts 10000 Monte Carlo steps[18]). It is interesting to notice that even if we assign to 20 % of the cells a random cell type in the initial condition, the sorting of the cell types keeps almost unchanged. Furthermore, even with a 40 % of cells characterized by a random cell type (in the initial condition), the sorting among cell types is only partially affected, for instance in regard to the appearance of minor invaginations of cells belonging to a specific cell type within the band of another one.

This outcome would suggest a substantial robustness of the cell sorting phenomenon even when exclusively based on differential adhesion properties.

6 Off-lattice (or lattice-free) models

1-, 2- and 3-dimensional *off-lattice* models of cell sorting in intestinal crypts and other biological systems have been developed over the years. Among them, there are several variants, mostly depending on the topological and geometrical representations used, other than simple discrete lattice. Some representations use a *center-based* approach,

[18] Time is measured in Monte Carlo steps (MCSs). One MCS consists of one index-copy attempt for each pixel in the cell lattice.

where each cell is labelled by the position in space of its nucleus (and/or other relevant features) and other geometrical and topological properties are derived from it: *Voronoi* representations (see, for instance, Fig. 6) and *deformable spherical* approximations fall in this category (cfr., references in the text below). Other approaches may use a direct polyhedral representation, where cells and their features are directly represented as surfaces and volumes. Once that a representation is chosen, then the equations describing, e.g., the adhesion forces among cells, are formulated and (numerically) solved by exploiting the particular representation structure and inter-cellular interactions.

One of the first models in this class was presented by Sulsky and Childress in Sulsky et al. (1984) and it was based on the Voronoi tessellation. During the last 10 years, starting with the work of Meineke et al. (2001), Drasdo (2000) and Hoehme and Drasdo (2010), more and more models have been proposed, mostly differing from each other in the basic underlying "cell representation". Lately, Galle et al. developed a bio-mechanical model (see below) and simultaneously, but independently, Drasdo on one side and Schaller and Meyer–Hermann on the other introduced distinct models that rely upon more physically plausible constraints.

We shall describe more carefully all these models in the following sections.

6.1 Meineke's model: the application of Voronoi tessellation

In Meineke et al. (2001), a 2-dimensional lattice-free model using Voronoi tessellation has been developed by Meineke et al. In this model cells are not restricted to stepwise motion within a grid. They move continuously under the influence of repulsive and attractive forces. Movement is maintained by means of the mitotic pressure originating from the bottom of the crypt: this increases the density of cells and, accordingly, the intensity of the repulsive forces. Besides, the combined effects of different forces in Meineke's model suggests that, as a consequence of the inhibition of the proliferation, cell motion continues temporarily until a steady-state cell distribution is reached. The crypt is still assumed to be cylindrical and, to represent the shape of the cells scattered on the surface, Voronoi polygons are used. The polygonal cell packing, based on the Voronoi tessellation, closely reproduces the morphology of the intestinal epithelium. It deserves noticing that Meineke's model is able to reproduce the same data as Loeffler's 2D-grid model (Loeffler et al. 1986) (see the beginning of Sect. 5), without assuming an age-dependent insertion rule for newly formed cells. In the lattice-free approach, daughter cells are randomly located at short distance from their parent cell and the cell boundaries are then recomputed: consequently most cell–cell contacts are preserved.

Parameters setting and validation

The setting of the various geometrical, kinetic and cell population-related parameters of the model is made on the basis of various studies published in Loeffler et al. (1986), Loeffler et al. (1988), Potten et al. (1988), Chwalinski and Potten (1989) and Paulus et al. (1993). The reference data set for the validation (on the general position of the cells, the position of the mitotic cells and the positional cell velocities) is taken from

Kaur and Potten (1986), the best fit being produced when cell migration in the crypt is a laminar flow.

6.2 Other models based on Voronoi tessellation

Besides Meineke's, other more general off-lattice models for epithelia have been introduced. In Morel et al. (2001), Voronoi tessellation has been used to describe a 2-dimensional longitudinal section of stratified epithelium. The model also considers an intracellular biochemical network that regulates cell proliferation, as well as extracellular factors that affect the system.

Other models including intracellular signaling pathways, have been developed by Smallwood et al. (2004) and Walker et al. (2004). These are 3-dimensional models that incorporate social behavior of cells: individual cells are represented as agents which respond to internal and external signals through predefined rules.

Parameters setting and validation

In regard to the model described in Morel et al. (2001) the estimation of most the parameters was realized on the basis of the work by Kohn (1998), while the role of a specific integrin in proliferation and adherence control is derived from Jensen et al. (1999). The validation of the results, with specific regard to the concentration of key molecules implicated in different phases of the cell cycle, is made by comparing with the results in Potten and Morris (1988) and Wright and Alison (1984).

6.3 Galle's bio-mechanical model

In a sequence of papers starting in 2005 (Galle et al. 2005, 2006a,b, 2009; Buske et al. 2011) Galle et al. published a 3-dimensional dynamic model for tissue organization and applied it to the crypts of the mouse small intestine. At variance with previous models, this one provides a bio-mechanical description of multicellular systems in which cells are thought of as deformable elastic bodies (keeping spherical shape) capable and free of moving, growing, dividing, differentiating and communicating with each other. The state of the multicellular system is labeled by the collection of (a) the cell positions (center of mass coordinates in the three-dimensional space), (b) the sizes of cells (the radii of spheres) and (c) an internal state vector $\boldsymbol{\Omega}$ for each cell recording internal activity status, e.g. the transcription of target genes of Wnt- and Notch pathway in the specific case of colonic crypts. The motion of cells is governed by *Langevin equations* which include different types of pairwise deterministic and stochastic forces.[19] The internal state vector can only be changed by the external cell dynamics (cell positions and size dynamics): there are not dynamical equations coupling the state vectors with the cell motion in the three-dimensional space. Such a link is only accounted for via constitutive relations. These relations express the dependence of cell internal activity

[19] Most of the simulation studies concerning intestinal crypt dynamics neglect stochastic components and are only build upon deterministic mechanical forces.

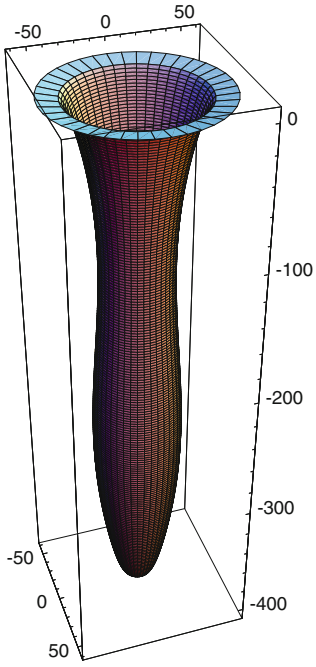

Fig. 5 Crypt substrate: geometric representation of a crypt in Galle's model

on the current position and size of the cell. The above mentioned deterministic forces can be divided as follows: *cell–cell interactions* and *cell–substrate interactions*. The substrate of the crypt is analytically approximated by a regular surface (see Fig. 5).

The cell–cell interaction consists of three contributions: adhesion, elastic deformation at the contact surface (Hertz model), volume elastic deformation (inflation or compression of the sphere) and frictional forces. Cells are assumed to interact with the basal membrane (substrate in Fig. 5) if their distance is lesser than their radius and they are removed from the crypt system if they lose contact with the basal membrane. The corresponding interaction energy is weakly adhesive above a threshold distance and repulsive below it, thus leading to a minimum configuration in which the cells are kept anchored to the substrate unless they abandon the crypt system.

Let $\boldsymbol{r}_i$ and R_i denote the position vector and radius of the i cell, then the cells move cooperatively according to the following system of coupled differential equations

$$\eta_{bm}\frac{d\boldsymbol{r}_i}{dt} + \sum_j \eta_c a_{ij}^c \left(\frac{d\boldsymbol{r}_i}{dt} - \frac{d\boldsymbol{r}_j}{dt}\right) = \boldsymbol{f}_i^{\text{det}} \tag{20}$$

$$\eta_v\frac{dR_i}{dt} + \sum_j \eta_c a_{ij}^c \left(\frac{dR_i}{dt} + \frac{dR_j}{dt}\right) = G_i^{\text{det}} \tag{21}$$

where η_{bm}, η_v are the friction coefficients at the cell–substrate contact and in course of a volume change of a cell, respectively; $\eta_c a_{ij}^c$ are the friction coefficients between

two cells in contact. Actually, a_{ij}^c is connected with the contact area as follows

$$a_{ij}^c = \pi \left[R_i^2 - \left(\frac{R_i^2 - R_j^2 + d_{ij}^2}{2d_{ij}} \right)^2 \right], \qquad d_{ij} = |\boldsymbol{r}_i - \boldsymbol{r}_j|. \tag{22}$$

The terms on the right-hand sides of (20) and (21) are the total forces on cell i

$$\boldsymbol{f}_i^{\text{det}} = \sum_j \frac{\partial H_{ij}}{\partial d_{ij}} \frac{(\boldsymbol{r}_i - \boldsymbol{r}_j)}{d_{ij}} + \sum_k \frac{\partial E_{ik}^{bm}}{\partial l_{ik}} \frac{(\boldsymbol{r}_i - \boldsymbol{\rho}_k)}{l_{ik}}, \qquad l_{ik} = |\boldsymbol{r}_i - \boldsymbol{\rho}_k| \tag{23}$$

$$G_i^{\text{det}} = \sum_j \frac{\partial H_{ij}}{\partial R_i} \tag{24}$$

where $\boldsymbol{\rho}_k$ denotes a point (a knot of a triangulation, see below) on the basal membrane (see Fig. 5). H_{ij} is the pairwise interaction energy between cell i and cell j and E_{ik}^{bm} the interaction energy between each cell and the basal membrane. The former is the counterpart of the CPM hamiltonian described above [see Eq. (5)] and it accounts for the contact and deformation forces mentioned above; the latter is the anchorage energy to the basal membrane. More precisely,

$$H_{ij} = W_{ij}^a + W_{ij}^D + W_i^K \tag{25}$$

where

$$W_{ij}^a = \varepsilon a_{ij}^c \tag{26}$$

is the adhesion energy (ε being the adhesion energy per unit contact area);

$$W_{ij}^D = \frac{2\left(R_i + R_j - d_{ij}\right)^{\frac{5}{2}}}{5D} \sqrt{\frac{R_i R_j}{\left(R_i + R_j\right)}}, \qquad D = \frac{3}{2}\left(\frac{1-\nu^2}{E}\right) \tag{27}$$

represents the deformation energy for contact and here E, ν are physical parameters of the cells representing Young modulus and Poisson ratio, respectively. Finally,

$$W_i^K = \frac{K}{2V_i^T}\left(V_i^T - V_i^A\right)^2, \tag{28}$$

with

$$V_i^A = V_i(R_i) - \sum_j \Delta V_{ij}^C, \quad V_i(R_i) = \frac{4}{3}\pi R_i^3, \tag{29}$$

$$\Delta V_{ij}^C = \frac{\pi}{3}\left[R_i - \left(\frac{R_i^2 - R_j^2 + d_{ij}^2}{2d_{ij}}\right)\right]^2 \left[2R_i - \left(\frac{R_i^2 - R_j^2 + d_{ij}^2}{2d_{ij}}\right)\right], \tag{30}$$

denotes the volume deformation energy, that is the energy corresponding to a change of volume in a cell and approximately taken to be a uniform compression or inflation energy of a sphere assuming a bulk elastic modulus K. Here V_i^T is the target volume (the volume of an isolated cell), V_i^A is the current volume, which is the volume of the sphere with actual radius R_i (this latter governed by a Langevin equation (21)) and corrected with the volume ΔV_{ij}^C of overlapping portions of neighboring cells. As for the basal membrane–cell interaction, it is modeled by a pairwise interaction potential where the pair involved consists of an individual cell and a knot of a triangulated fiber network which discretizes the basal surface given in a closed analytical form as follows

$$\varrho\,(z) = \varrho_0 \left[1 + \lambda_1 \cos\left(2\pi \frac{z}{z_0} + \frac{\pi}{2}\right)\right] \sqrt{\frac{2}{\pi} \arccos\left(\left(\frac{z}{z_0}\right)^{\lambda_2}\right)}, \tag{31}$$

where $\varrho(z)$ is the radius of the crypt at the height z, i.e. at the distance from the top (crypt-villus junction, $z = 0$) and λ_1 and λ_2 are shape parameters (see Fig. 5).[20] The interaction energy is assumed to be

$$E_{ik}^{bm} = \frac{\varepsilon^{knot}}{N_i^{knot}} \left(\omega \ln\left(\frac{l_{ik}}{R_i}\right) - \frac{l_{ik}}{R_i}\right), \tag{32}$$

where ε^{knot}, N_i^{knot} represent the interaction energy per knot and the number of knots in interaction with the cell i, respectively; ω is a scaling factor. Clearly, the interaction energy [Eq. (32)] keeps the cells close to the substrate at a minimum distance provided that l_{ik} is smaller than the radius R_i, otherwise no interaction exists.

The cell-cycle is actually taken to be pre-programmed in Galle's model and, since cells are not isolated but strongly interacting with each other, the *projection* of the internal processes onto the external dynamics has to be considered. In the model, cell–cell and cell–substrate adhesion are assumed to be dominated by interactions of different cell adhesion molecules (receptors) with their ligands. It is assumed that these receptors (ligands) are uniformly distributed on the cell surface and that the substrate consists of a dense film of ligands. The inter-cellular dynamics is eventually studied on timescales much larger than the intrinsic timescale for receptor-ligand binding. Actually the energy constant ε in Eq. (26) is depending on the density of receptors and ligands on cell surface. Furthermore, Galle's model accounts for cell growth, division and differentiation according to predefined rules stemming from experimental studies. As for the cell-cycle, in the interphase any cell is assumed to increase its target volume by stochastic increments. The increase of V_i^T results in an increase of the compression energy [Eq. (28)] and, accordingly, in a force transmission (pushing forward) to the surrounding cells. Subsequently, the current volume V_i^A in Eq. (28) adapts to V_i^T almost continuously. The internal cell dynamics is thus projected onto the external one

[20] Notice that Eq. (31) can reproduce a cylinder-like surface upon choosing appropriate values of the shape parameters. On the other hand, the bottom of such surface keeps being closed for any choice of the parameters.

by conveying internal stimuli and process outcomes to external mechanical stimuli of one cell to another close to it. The time needed for a cell to double its target volume is the cell growth time.

Cell growth also depends on the environment and this interaction is simulated by introducing 3 different mechanisms of control and regulation of growth: (a) a cell with a volume below a threshold value is assumed to be too much compressed by the surrounding cells so that its growth is inhibited; (b) a minimal contact area between a cell and the substrate is required for the cell to enter the cell cycle and growth accordingly, thus leading to an anchorage-dependent growth; (c) if the contact area decreases below a prescribed value, the cell undergoes a programmed death.

In intestinal crypts, activation of the Wnt- and Notch-pathways was demonstrated to be essential for stem cell maintenance as well as proliferation and differentiation (see Sect. 2). Galle et al. assume that proliferation and differentiation strictly depend on the activation of Wnt- and Notch-pathways. In greater detail, the Wnt-activity spatial gradient is related to the local curvature of the basal membrane and to the cell position, while Notch-signaling is ruled by the lateral inhibition mechanism and depends on the number and types of cell–cell contacts. These assumptions are modeled by the status vector $\boldsymbol{\Omega}$ mentioned above describing the internal activity and not governed by dynamical equations. The activity status is the transcription of target genes of the Wnt- and Notch-pathway denoted by I_{Wnt} and I_{Notch}, respectively. The former is assumed to be a function of the position along the axis of the crypt and, accordingly, of the curvature of the substrate. The latter is calculated through cell–cell contact: a cell is Notch-activated by all cells in contact with it and expressing Notch-ligands. Lineage specification is then modeled on the basis of specific combinations of the activation levels of Wnt- and Notch pathways.

The outcome of Galle's model simulations are: homeostasis, spatio-temporal self-organization, cell migration and re-arrangement. Moreover this study includes sensitivity, stability and flexibility against changes in the Wnt and Notch signaling activation levels. In particular, self-organization of the intestinal crypt cells depends on the assumption of the externally assigned Wnt spatial gradient.

Parameters setting and validation

With particular regard to the latest development of the model (Buske et al. 2011), the various parameters of the model[21] were set, according to the cases, on the basis of measured properties of the crypt shape (Potten and Loeffler 1990), fit on different know biological and biochemical data (Marshman et al. 2001; Galle et al. 2005; Ireland et al. 2005) or estimated (see Table 1. in Buske et al. 2011 for the complete description of the parameters set).

The behaviour of the model was proven to correctly reproduce qualitative experimental findings, in regard to a large range of phenomena (see above), while quantitative agreement is based on detailed fitting. In particular, the model is capable of quantitatively reproduce numerous phenomena, such as: steady state cell production, average

[21] Distinguishable in (i) parameters of the cell model, (ii) parameters of the basal membrane model, (iii) parameters of crypt dynamics and (iv) parameters of the lineage specification and differentiation model.

spontaneous apoptosis rate (Marshman et al. 2001), distribution of LGR-5 positive cells (Barker et al. 2007), spatial distribution of the cells (Bjerknes and Cheng 1981; Chwalinski and Potten 1989; Paulus et al. 1993), clonal competition (Li et al. 1994; Winton and Ponder 1990), deregulation of Wnt and Notch signaling pathways (Samson et al. 2004; Andreu et al. 2005; Free et al. 2005; Fevr et al. 2007; van Es et al. 2005), robustness to perturbations on subpopulations of cells (van der Flier et al. 2009).

6.3.1 Further developments

As stressed by Galle in his work (Buske et al. 2011), the curvature of the membrane substrate (Fig. 5) is important for the overall dynamics, especially in connection with cancer development inside the crypt. To account for this, a reasonable model could point at integrating Wong et al.'s model of crypt dynamics with Hogeweg model of nutrients' diffusion and reaction (Wong-PDE) in three dimensions including the non-zero curvature (gaussian curvature) of the substrate. In this regard the basic question to address would be: how to implement CPM on a non-cylindrical crypt, as for example Galle's crypt surface (Fig. 5)?

6.4 The work of Schaller and Meyer–Hermann

Starting also a few years ago and simultaneously with the above outlined Galle's model, Schaller and Meyer-Hermann (2005) put forward a variant of Galle's model based on the Voronoi tessellation to describe epithelial sheets (Sulsky et al. 1984); more recently Kempf et al. (2010) reused and modified the model to describe cell-dynamics in spheroidal tumors. Schaller–Meyer-Hermann's model is a hybrid three-dimensional biomechanical agent-based Voronoi–Delaunay model of general multicellular systems. In this model, the single cell is a quasi-spherical deformable body: its shape varies from spherical in thin solutions to convex polyhedral in dense tissues.[22] The cells interact with their next neighbors and these latter are determined by a weighted Delaunay triangulation. Similarly to Galle's model the cellular interactions include elastic cell–cell forces, cell–cell and cell–substrate adhesive forces and friction forces between cells and the cells and the substrate. In particular, the adhesion strength depends on the concentrations of receptors and ligands on the surface of the cellular membrane. The external coordinates of each cell include accordingly the position and an effective radius, this latter determined by the shape of the cell (whether a sphere or a Voronoi polyhedron). The cell internal status is also taken into account and used to record the receptor and ligand concentration on the cellular membrane (necessary for the adhesion), the internal clock for the prescribed cell-cycle and the cell-type-specific coupling constants for both elastic and adhesive interactions.

[22] At a first glance, the polyhedral shape could appear as a mathematical abstraction in order to simplify the model. Actually, in recent experiments (Dubois et al. 2001) the spontaneous formation of hollow bilayer vesicles with polyhedral symmetry has been observed. On the basis of the experimental phenomenology it was suggested (Dubois et al. 2004) that the mechanism for the formation of bilayer polyhedra is minimization of elastic bending energy (Haselwandter and Phillips 2011).

The dynamics is dictated by over-damped Newton equations (the inertial term is neglected in comparison with the frictional forces) and a system of ordinary differential equations is obtained similar to the one in (20) and (21). In addition, the spatio-temporal distribution of two nutrients (oxygen and glucose) is described by reaction-diffusion equations as in (15) and similar equations above in the same spirit of the Glazier–Graner–Hogeweg model described above. Cells consume nutrients which are converted into biomass by so increasing the cell size. Comparisons with experimental results is considered in order to set up the rates of diffusion and reaction. As for the cell-cycle, the model includes proliferation according to predefined rules and simulations are performed in order to study the mechanisms for induction of cell necrosis. The target of the study is to investigate the tumor spheroid morphology in a given tissue. The direct application to intestinal crypts has not been considered yet.

Parameters setting and validation

The setting of the parameters is exhaustively described in Table 1 of Schaller and Meyer-Hermann (2005) and is based on various data regarding physical, biochemical and biological properties of real cells (Landry et al. 1981; Freyer and Sutherland 1986; Casciari et al. 1992; Galle et al. 2005).

The results on proliferation and growth showed some unexpected phenomena already observed in experiments (Landry et al. 1981). The results on oxygen and glucose uptake were proven to be within the range observed in literature (e.g. Freyer and Sutherland 1986; Kunz-Schughart et al. 2000; Wehrle et al. 2000). Moreover, the evolution of the overall cell number were validated with (Freyer and Sutherland 1986), while the results on the morphology of the tumor spheroid with (Casciari et al. 1992).

6.4.1 Further developments

In light of Schaller–Meyer-Hermann's mathematical model, a reasonable extension of it could be a combination of Galle's model of intestinal crypt dynamics with the representation of cells in terms of Voronoi polyhedra and Delaunay triangulation.

6.5 Computational tools for lattice-free models: CHASTE

Very recently a novel software (Cancer, Heart And Soft-Tissue Environment, CHASTE) has been designed by implementing an agent-based model for crypt dynamics. The authors of Pitt-Francis et al. (2009) model the crypt as a monolayer of cells moving along a cylindrical surface. The crypt is as usual rolled out onto a plane and periodic boundary conditions are imposed along the sides of the rectangular domain. The model basically includes four main components.

1. A first component simulates the Wnt signaling pathway;
2. A second component includes a cell-cycle model which, together with the information from the Wnt signaling pathway, determines when cells are ready to divide and differentiate.

3. A third component is in charge for cell migration at a macro-scale level via a mechanical model as the ones described above (Galle's and Schaller–Meyer-Hermann's models).
4. A fourth component is a PDE solver for the solution of reaction-diffusion PDEs which model the diffusion and the uptake of particular nutrients (oxygen and glucose), with the cell model being dependent on the local nutrient concentration.

As for the first and second components, in the CHASTE model every cell is endowed with its own cycle model which can be influenced by the external environment. It is known that the proliferative activity along the axis of the crypt goes from an intense one at the bottom and decreases as long as the top of the crypt is reached. The proliferation is actually correlated with the presence of a spatial gradient of extracellular Wnt factors (see Sect. 2). A spatial gradient of Wnt is therefore imposed in the model with high levels of Wnt at the crypt base and low levels at the top. A model is used to calculate the corresponding position-dependent levels of gene expression via a system of nonlinear ordinary differential equations (van Leeuwen et al. 2007). The outcome of this calculation is then used to determine the cell-cycle as a function of the position along the crypt axis: close to the bottom the cells are exposed to high levels of Wnt and the cycle is enhanced; at the top no division occurs. The third component deals with the external mechanical model.

A Voronoi tessellation-based cell-centre approach is used in which the centers of neighboring cells are connected by linear springs and a Delaunay triangulation is performed at each time step in order to find the cells which are connected (see Fig. 6). If $\boldsymbol{r}_i$ denotes the centre of the cell i, the intercellular force between cell i and cell j is taken to be

$$\boldsymbol{f}_{ij} = \beta \left(|\boldsymbol{r}_i - \boldsymbol{r}_j| - s_{ij} \right) \frac{\boldsymbol{r}_i - \boldsymbol{r}_j}{|\boldsymbol{r}_i - \boldsymbol{r}_j|}, \tag{33}$$

where β is the elastic constant and s_{ij} is the natural length. The dynamics is governed by over-damped Newton equations where the cell viscosity models the cell–substrate adhesion. The natural length s_{ij} is taken to be the diameter of the cells. When a cell divides, according to its internal cell-cycle model, a new cell is placed at a smaller distance than s_{ij} from the mother cell and the new s_{ij} of the cells which have just divided is increased linearly over the course of one hour up to the mature length. All this is done in order to simulate the mitosis. In this way the cell-cycle influences the external intercellular mechanics and cell movement, and , in turn, the cell-cycle is influenced by the Wnt-gradient calculated as a function of the position along the crypt axis.

One of the first interesting results obtained through CHASTE was to show that if stem cells are forced to reside at the base of the crypt, the dynamical evolution leads toward the formation of a polyclonal crypt, while if stem cells are supposed to have no spatial constraints, the crypt eventually becomes monoclonal.

Furthermore, the system was proven to be capable of effectively describing the dynamics of multicellular tumour spheroids (Pitt-Francis et al. 2009).

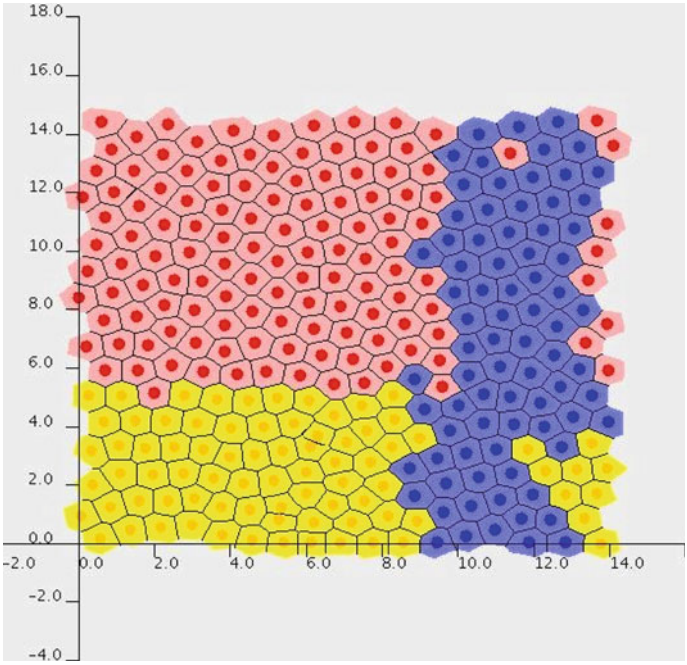

Fig. 6 Screenshot of a typical CHASTE simulation of intestinal crypt. In detail, the crypt is modeled on a cylindrical geometry with periodic boundary condition and the cells are represented as Voronoi polygons. *Yellow* cells are those in transit amplifying stage, *red* cells are differentiated cells, while *blue* cells are the progeny of a single cell present at the beginning of the simulation (taken from http://www.cs.ox.ac.uk/chaste/) (color figure online)

7 Libraries, interoperability, repositories and software

In moving towards a conclusion of this review, in this section we discuss more generally the important issue of software for the implementation of the presented mathematical and computational models.

With the proliferation of software tools and libraries for multicellular systems modeling, a need is arising for testing, validating and exchanging models and results. This process is not new in the various bioinformatics, systems biology and computational biology communities, as over the past ten or fifteen years, several efforts have appeared in various *niches*, meeting various degrees of success.

Libraries, interoperability layers, repositories and software (in brief: "the tools") solve different problems for different researchers, but they can now be broadly classified into three categories: (1) *simulation and analysis tools*, (2) *query and database tools*, and (3) *exchange formats*. The tools span different dimension scales,[23] where the most pertinent subdivision for the sake of this review is the separation between the *intra*-cellular, *inter*-cellular levels, upward towards the "organ" level.

[23] …and here we limit ourselves to the "biological" space-time scales; excluding, e.g., the scales pertaining to actual physical molecular interactions that are the province of computational chemistry.

The most active researchers' communities producing "the tools" have arguably been those working at the intra-cellular (often at the single-cell) level. In this respect, the number of simulation environments for *reaction systems* of metabolic and regulatory systems based on ODE/PDE, SDE, Monte Carlo (i.e., Gillespie's) (Gillespie 1976, 1977; Gibson and Bruck 2000) approaches and their variations and intermixing is quite large; we do not list any here, for the lack of space. Within these communities several repositories of information have appeared and are now public: we group them in *pathway databases* and *models databases*, with a non-null intersection. Some of the now canonical resources in this categories are KEGG (http://www.genome.ad.jp/kegg/), Reactome (Stein 2004), Pathway Commons (Cerami et al. 2006). "Models repositories" contain published models which are curated and annotated; we cite the BioModels repository (Le Novère et al. 2006; Li et al. 2010) and the models section of the CellML (CellML 2001; Cuellar et al. 2003). Many of these efforts rely on exchange formats based on XML, and while defining *XML-4-something* has become a cottage industry, three efforts have stood out over the last 10 years or so: SBML (System Biology Markup Language 2002), CellML (Cuellar et al. 2003) for the exchange of "executable" models and BioPax (http://www.biopax.org) for the exchange of pathway informations; all these standards do reuse many efforts put forth by researchers who developed *ontologies* for the annotation of and reasoning over biological data; the Gene Ontology (Gene Ontology Consortium 2006) is the best known example and the OBO Foundry (Smith et al. 2007) is a reasoned collection of many specialized ontologies covering a lot of terrain in the biology and medicine. Around these "standards" an ecosystem of applications and other layered standards is developing. E.g., the SED-ML (Köhn and Novère 2008) is a recent specification with the goal of providing a standardized way to describe "simulation experiments"; the companion *Systems Biology Results Markup Language (SBRML)* (Dada et al. 2010) aims at describing "simulation results".

Going back to the topic of this review, we observe that most of the current computational models of biological systems (those that can be defined "reaction level-based") usually deal with single cell environments and/or a well mixed mixtures of the molecular species involved in a specific phenomenon. One of the major differences of the approach of multi-cellular systems modeling and simulation is the attention on the key role played by the *topological* and therefore *geometrical* arrangement of each cell in space (and in time), which is usually not considered. This is also the reason why we decided to concentrate on the distinction between in-lattice and off-lattice models.

Geometrical information is heavily used in (mostly) *Finite Element Analysis* tools like those collected in the SimTk site (https://simtk.org), which deal essentially with organ and musco-skeletal systems. CompuCell3D (Sect. 5.5) and Chaste (Sect. 6.5) do obviously use geometrical information, yet at the time of this writing only a few efforts have appeared with proposals to standardize an exchange format specifically tailored to multi-cellular systems, as some consensus has emerged that such systems have some peculiarities arising from the combination of topology, geometry and biology that is being studied. To this end, the so called *Spatial extension package* of SBML (Schaff 2011) and the FieldML specification (Christie et al. 2009) provide a groundwork upon which geometrical extensions can be built; yet, it appears that both

approaches will need carefully crafted extensions to fully accomodate fully multicellular dynamics.

At a recent workshop on Multicellular Modeling (Monk and Owen 2011) in Nottingham (U.K.) the participants presented several tools and discussed proposals for various exchange formats. Among the other systems not directly related to the simulation of colonic crypts we can cite OpenAlea (Pradal et al. 2008) and Subcellular Element Model (Sandersius et al. 2011). An exchange format targeting multi-cellular systems, MultiCellXML (Macklin et al. 2010) is being put forth by a group at University of Dundee in the U.K. A result of the Nottingham meeting was a preliminary set of guidelines for an exchange format capable of accommodating different modeling strategies and for different multicellular systems. The main idea behind such guidelines is to classify models based on the *in-lattice/off-lattice* partition, a separate description of the *topology* and of the *geometry* of the multicellular system, and on the notion of *maps* and *embedding* of cells and other structures in such entities.

8 Towards a framework for the classification and evaluation of mathematical and computational models of intestinal crypts and CRC

The computational models we have presented in this review all share some common characteristics; the principal one being the casting of most phenomena and thus their related computations in terms of *energy relationships*. While this is an excellent organizing paradigm, which does play an unmistakable role in the dynamics of biological systems at any scale, its use so far has somewhat escaped Sydney Brenner's invocation (Brenner 1999):

> *…this must not simply be another way of describing the behavior. For example it is quite easy to write a computer program that will produce a good copy of worms wriggling on a computer screen. But the program, …has nothing in it about neurons or muscles. …. A proper simulation must be couched in the machine language of the object, in genes, proteins and cells.*
>
> *…I want the new information embedded into biochemistry and physiology in a theoretical framework, where the properties at one level can be produced by computation from the level below.*

While new computational developments may get us closer to this goal, thanks especially to new parallel programming advances (most notably GPU programming), it is necessary to ensure that simulation models are grounded in the corpus of data collected by biologists over the years.

In this regard, in Tables 1 and 2 we propose a possible first assessment criterion of the reviewed models, based on the capability of *qualitatively* describing the distinct biological phenomena involved in the activity of the colonic crypts, both in the normal and in the aberrant development.

While such classification is important to categorize each model, an evaluation of the models w.r.t. their ability to *quantitatively* explain published data and biological pro-

Table 1 Classification of the reviewed in-lattice models according to the description of the essential biological processes involved in the normal and in the transformed development of the crypts and of other multicellular systems

	GGH	W	SH	H1	H2	SS	S
Normal tissue							
General phenomena	×	×	×	×	×	×	×
Dynamic turnover	×	×	×	×	×	×	×
Cell differentiation		×		×	×	×	×
Pathways		×	×		×	×	×
Transformed tissue							
General phenomena		×					×
Mod. in cell types							×
Mod. in pathways		×					×
Inter. with other tissues							×

The rows are labeled according to the classification presented in Sect. 3 and the marker "×" denotes the actual or potential capability of each specific model in modeling at least a part of the biological phenomena included in each class. The columns are labelled with the initials of the authors of the relative model
GGH Graner and Glazier (1992, 1993), *W* Wong et al. (2010), *SH* Savill and Hogeweg (1997), *H1* Hogeweg (2000), *H2* Hogeweg (2000, 2002), *SS* Savill and Sherratt (2003), *S* Shirinifard et al. (2009)

Table 2 Classification of the reviewed off-lattice models according to the description of the essential biological processes involved in the normal and in the transformed development of the crypt and of other multicellular systems

	Me	Mo	G	SMH	C
Normal tissue					
General phenomena	×	×	×	×	×
Dynamic turnover	×	×	×	×	×
Cell differentiation	×	×	×	×	×
Pathways		×	×	×	×
Transformed tissue					
General phenomena		×		×	×
Mod. in cell types				×	×
Mod. in pathways		×		×	×
Inter. with other tissues		×			×

Me Meineke et al. (2001), *Mo* Morel et al. (2001), *G* Galle et al. (2005, 2006a,b, 2009); Buske et al. (2011), *SMH* Schaller and Meyer-Hermann (2005), *C* Pitt-Francis et al. (2009)
The rows are labeled according to the classification presented in Sect. 3 and the marker "×" denotes the actual or potential capability of each specific model in modeling at least a part of the biological phenomena included in each class. The columns are labelled with the initials of the authors of the relative model

cesses is also needed, in order to foster the creation of a framework which could serve as a "validation" and "comparison" scaffold. More ambitiously, one important future target is the development of a general conceptual framework capable of evaluating the

models, w.r.t. their *predictive power*, which is the overall goal of "modelers" worldwide.[24]

To this end, along this review we have systematically provided additional comments on the setting of the parameters of the models and their validation, based on various experimental data, often obtained by means of experiments *ad hoc* designed.

Nonetheless, we would like to stress that the amount of published data contained in various databases is, by the time of this writing, enormous (see Sect. 7), and most of the data contained in the public repositories is not related to "models" or "simulations", but to *sequence data* (DNA, RNA, miRNA, protein, etc.), their relations (e.g., protein-protein interaction data), and other genomic measurements, e.g. in the form of *gene expression data* (e.g., the result of micro-array experiments or copy-number data). Most of this data is accessible through several "portals", like ENTREZ (http://www.ncbi.nlm.nih.gov/entrez/) and EMBL- EBI (http://www.ebi.ac.uk/): one exemplar data-base of gene expression profiles is the *Gene Expression Omnibus* (GEO) (Barrett et al. 2010). Image data is also extremely important in the validation tasks carried out by the groups whose work we reviewed and there are imaging data bases that are becoming useful as a source of data (see, for example, Martone et al. 2008).

Just considering gene-expression data,[25] we observe that it should be possible to design a simulation model to "track" data contained in GEO. For example, one undertaking of our group is to ensure that our simulators take into account the data analyzed by Reid et al. (2009); this data set can be organized in a temporal axis, e.g., by observing the variation of copy-number counts, and gene-expression relationships can be reconstructed using the algorithms presented in Ramakrishnan et al. (2010). The resulting gene-expression relationship data could be cross-checked with simulation results that tracked a subset of gene products "of interest". Such an approach could be applied to each new model and/or simulator appearing in the literature.

More in general, the capability of describing complex biological systems from both the qualitative and the quantitative point of view should represent the benchmark for any future model targeting colonic crypts and CRC development, as well as for the overall computational and translational cancer research (as proposed, for instance, in Mathew et al. 2003).

9 Conclusions and future research

The main goal of this review was to present an up-to-date landscape of the spatial computational modeling approaches designed (or suitable) for an effective description of the intestinal crypt morphology and morphogenesis, with particular regard to the subsequent characterization of the development of the CRC. In this regard, we have shown that all the distinct models present several interesting features and numerous differences, allowing to describe the phenomenology of the crypts according to

[24] It should be immediately clarified, that ours is mostly a *conceptual* and *methodological* proposal stemming from our previous experiences; it is neither complete not fully tested. We are actively working on the subject and would simply like to circulate our overall approach, inasmuch as we find value in it.

[25] Similar considerations could be made about sequence data, especially given the recent advances in *Next Generation Sequencing* (NGS) (Mardis 2008).

different perspectives (see Tables 1 and 2). Perhaps, what is still missing is a general model that covers all the distinct processes and phenomena involved in the crypt activity, providing a possibly exhaustive and coherent picture of the overall dynamics, based on a holistic system-based approach.

To this end one of the most suitable and effective methodological frameworks is that provided by *multi-scale modeling* techniques which exploit the rightly presumed (and observed) *separation of time-scales* of several phenomena at the cellular level. In this way it will be possible to cover and characterize all the hierarchical levels of the crypt organization, from molecules to tissue. The integration of the sub-cellular level (gene regulation, intra-cellular communication), the cellular level (signaling pathways, inter-cellular communication, cell–environment communication) and the tissue level (spatial patterning, movement and migration, crypt homeostasis) within a coherent computational model could be an important (and admittedly very ambitious) goal for the next future. Of course, exploiting such separation of times-scales will also allow for an almost natural partitioning of the simulation problems across a parallel and/or distributed computer architecture. In this respect, the MAPPER project (Multiscale Applications on European e-Infrastructures 2010) and the MML proposal (Falcone et al. 2010), alongside many other grid-based computation distribution schemes, represent a set of technologies of interest for multi-cellular simulations.

In this regard, our current efforts are mainly aimed at the development of a multi-scale computational model that may integrate a general model of gene regulatory network (GRN) with a morphological model of crypt dynamics (as those described in the current review, or possible evolutions). The model was introduced in a preliminary version in Graudenzi et al. (2012).

More in detail, the model of *noisy random Boolean networks* (NRBN) is a highly abstract[26] dynamical model of gene regulatory network (Peixoto and Drossel 2009; Serra et al. 2010) (an evolution of the original RBN model Kauffman 1969a,b, 1995), which was proven to reproduce several dynamical properties of real networks, with particular regard to the differentiation process (Villani et al. 2011). This GRN model will account for the internal (also defined as *low-level*) dynamics of the cells in the crypt. In particular, a specific NRBN will be associated to each cell of the crypt and the essential cellular processes, i.e. cell growth, division and differentiation will be then modeled through the association with the emerging *dynamical* behaviour (hence, not prefixed as in most of the reviewed models). The key structural features of the networks (i.e. topology, updating functions, sub-networks, etc.) will be based on the existing (yet still partial) available data and mappings on real gene regulatory networks (e.g. Davidson et al. 2002; Lee et al. 2002; Wagner 2002; Basso et al. 2005; Olson et al. 2006; Heckera et al. 2009) and will be integrated with an explicit representation of the signaling pathways and of the inter-cellular communication processes (as proposed, for instance, in Kirouac et al. 2010; Damiani et al. 2011) that are known or supposed to be directly involved in the crypt activity (see the references in Sect. 2.3).

This low-level dynamics will eventually steer the (high-level) spatial dynamics of the crypts (modeled through one of the overviewed models such as, for example,

[26] i.e. not referring to any specific organism or cell type.

the Cellular Potts Model) with specific regard to cell sorting, migration and niche maintenance phenomena, and will determine its general behavior, homeostasis and fate.

One of the main advantages of this approach resides in the possibility of simulating the impact on the general activity of the crypt of different kinds of perturbations and damages at the low-level, such as (a) the occurrence of distinct genetic mutations in one or more cells, (b) possible damages or disruptions of the signaling pathways, (c) the presence of biological "noise", (d) the changes in the environmental conditions, with obvious reference to the appearance and the development of cancer. Genomic databases on cancer such as, e.g., *The Cancer Genome Atlas* (The Cancer Genome Atlas), will be the essential for the validation of the model.

Acknowledgments We wish to thank the Regione Lombardia for its support of this research under the projects RETRONET and NETWORK ENABLED DRUG DESIGN (NEDD). Our thanks go also to Prof. Giancarlo Mauri for his continuos support and encouragement, to Giulio Caravagna and Silvia Crippa for the helpful discussions, to Dr. Manuela Gariboldi of IFOM-IEO and Istituto Nazionale dei Tumori in Milan for her inspiration to work on the specific topic of colorectal cancer, to Prof. Gary Bader of the University of Toronto for his gracious agreement to participate in the long term project, to Giulia Begal for kindly designing the images, to Dr. Markus Owen of Nottingham University for having organized the Multicellular Workshop 2011 where several community issues about modeling and model exchange were discussed, and to the Department of Informatics, Systems and Communication of the University of Milan Bicocca for the overall support given to the RETRONET project. Finally, G.D.M wishes to acknowledge for financial support of this work the Programma "Dote Ricercatori per lo sviluppo del capitale umano nel Sistema Universitario Lombardo"—Programma Operativo Regionale—Ob.2 Asse IV—FSE 2007-2013.

References

Adams J, Cory S (2007) The bcl-2 apoptotic switch in cancer development and therapy. Oncogene 26: 1324–1337

Adams J, Watt F (1989) Fibronectin inhibits the terminal differentiation of human keratinocytes. Nature 340:307–309

Alberts B, Johnson A, Lewis J, Raff M, Roberts K, Walter P (2007) Molecular Biology of the Cell, 5th edn. Garland Science, New York

Andreu P et al (2005) Crypt-restricted proliferation and commitment to the paneth cell lineage following apc loss in the mouse intestine. Development 132:1443–1451

Andreu P et al (2008) A genetic study of the role of the wnt/-catenin signalling in paneth cell differentiation. Dev. Biol. 324:288–296

Armstrong P (1989) Cell sorting out: the self-assembly of tissues in vitro. Crit Rev Biochem Mol Biol 24:119–149

Armstrong P, Parenti D (1972) Cell sorting in the presence of cytochalasin b. J Cell Biol 55:542–553

Arvanitis D, Davy A (2008) Eph/eprhin signaling: networks. Genes Dev 22:416–429

Barker N et al (2007) Identification of stem cells in small intestine and colon by marker gene lgr5. Nature 449:1003–1007

Barker N, Ridgway R, van Es J, van de Wetering M, Begthel H, van den Born M, Danenberg E, Clarke A, Sansom O, Clevers H (2009) Crypt stem cells as the cells-of-origin of intestinal cancer. Nature 457:608–611

Baron M (2003) An overview of the notch signalling pathway. Semin Cell Dev Biol 14:113–119

Barrett T, Troup DB, Wilhite SE, Ledoux P, Evangelista C, Kim IF, Tomashevsky M, Marshall KA, Phillippy KH, Sherman PM, Muertter RN, Holko M, Ayanbule O, Yefanov A, Soboleva A (2010) NCBI GEO: archive for functional genomics data sets–10 years on. Nucleic Acids Res 39(Database):D1005–D1010

Basso K et al (2005) Reverse engineering of regulatory networks in human b cells. Nature Genetics 37: 382–390

Batlle E et al (2002) Beta-catenin and tcf mediate cell positioning in the intestinal epithelium by controlling the expression of ephb/ephrinb. Cell 111:251–263
Bienz M, Clevers H (2000) Linking colorectal cancer to wnt signaling. Cell 103:311–320
Bjerknes M (1996) Expansion of mutant stem cell populations in the human colon. J Theor Biol 178: 381–385. doi:10.1006/jtbi.1996.0034
Bjerknes M, Cheng H (1981) The stem-cell zone of the small intestinal epithelium. ii. Evidence from paneth cells in the newborn mouse. Am J Anat 160:165–175
Boland C (2002) Heredity nonpolyposis colorectal cancer (hnpcc). In: Vogelstein B, Kinzler KW (eds) The Genetic Basis of Human Cancer, 2nd edn. McGraw-Hill, New York, pp 307–321
Boman B, Fields J, Bonham-Carter O, Runquist O (2001) Computer modeling implicates stem cell overproduction in colon cancer initiation. Cancer Res 61:8408–8411
Booth C, Brady G, Potten C (2002) Crown control in crypts. Nat Med 8:1360–1361
Bourgin C, Murai K, Richter M, Pasquale E (2007) The epha4 receptor regulates dendritic spine remodeling by affecting 1-integrin signaling pathways. J Cell Biol 178:1295–1307
Brenner S (1999) Theoretical Biology in the Thurd Millenium. Philos Trans R Soc Lond B 354:1963–1965
Brown S, Riehl T, Walker M, Geske M, Doherty J, Stenson W et al (2007) Myd88-dependent positioning of ptgs2-expressing stromal cells maintains colonic epithelial proliferation during injury. J Clin Invest 117:258–269
Bunow B, Kernevez J, Joly G, Thomas D (1980) Pattern formation by reaction-diffusion instabilities: application to morphogenesis in drosophila. J Theor Biol 84:629–649
Burgess P et al (1997) The interaction of growth rates and diffusion coefficients in a three-dimensional mathematical model of gliomas. J Neuropathol Exp Neurol 56:701–713
Buske P, Galle J, Barker N, Aust G, Clevers H, Loeffler M (2011) A comprehensive model of the spatio-temporal stem cell and tissue organisation in the intestinal crypt. PLoS Comput Biol 7(1):e1001,045. doi:10.1371/journal.pcbi.1001045
Casciari J, Sotirchos S, Sutherland R (1992) Variations in tumor cell growth rates and metabolism with oxygen concentration, glucose concentration, and extracellular ph. J Cell Physiol 151:386–394
CellML (2001) http://www.cellml.org
Cerami EG, Bader GD, Gross BE, Sander C (2006) cPath: open source software for collecting, storing, and querying biological pathways. BMC Bioinformatics 7. doi:10.1186/1471-2105-7-497
Chen C et al (1997) Geometric control of cell life and death. Science 276:1425–1428
Christie GR, Nielsen PMF, Blackett SA, Bradley CP, Hunter PJ (2009) FieldML: concepts and implementation. Philos Trans R Soc 367:1869–1884. doi:10.1098/rsta.2009.0025
Chwalinski S, Potten C (1989) Crypt base columnar cells in ileum of bdf1 male mice-their numbers and some features of their proliferation. Am J Anat 186:397
Clevers H, Battle E (2006) Ephb/ephrinb receptors and wnt signaling in colorectal cancer. Cancer Res 66:2–5
Coussens L, Werb Z (2002) Inflammation and cancer. Nature 420:860–867
Crosnier C, Stamataki D, Lewis J (2006) Organizing cell renewal in the intestine: stem cells, signals and combinatorial control. Nat Rev Genet 7:349–359
Cuellar AA, Lloyd CM, Nielsen PF, Bullivant DP, Nickerson DP, Hunter PJ (2003) An overview of CellML 1.1, a biological mdel description language. Simulation Trans Soc for Model Simul Int 79(12):740–747
Dada JO, Spasić I, Paton NW, Mendes P (2010) SBRML: a markup language for associating systems biology data with models. Bioinformatics 26(7):932–938
Damiani C, Serra R, Villani M, Kauffman S, Colacci A (2011) Cell–cell interaction and diversity of emergent behaviours. IET Syst Biol 5(2):137–144
Davidson E et al (2002) A genomic regulatory network for development. Science 295:1669
Deroanne C, Vouret-Craviari V, Wang B, Pouysségur J (2003) Ephrina1 inactivates integrin-mediated vascular smooth muscle cell spreading via the rac/pak pathway. J Cell Sci 116:1367–1376
Di Garbo A, Johnston MD, Chapman SJ, Maini PK (2010) Variable renewal rate and growth properties of cell populations in colon crypts. Phys Rev E 81(6):061909. doi:10.1103/PhysRevE.81.061909
D'Onofrio A, Tomlinson I (2007) A nonlinear mathematical model of cell turnover, differentiation and tumorigenesis in the intestinal crypt. J Theor Biol 244:367–374
Dover R, Potten C (1988) Heteogeneity and cell cycle analyses from time-lapse studes of human keratinocytes in vitro. J Cell Sci 89:359–364
Drasdo D (2000) Buckling instabilities in one-layered growing tissues. Phys Rev Lett 84(19):4244–4247

Dubois M, Demè B, Gulik-Krzywicki T, Dedieu JC, Vautrin C, Dèsert S, Perez E, Zemb T (2001) Self-assembly of regular hollow icosahedra in salt-free catanionic solutions. Nature 411:672–675. doi:10.1038/35079541

Dubois M, Lizunov V, Meister A, Gulik-Krzywicki T, Verbavatz JM, Perez E, Zimmerberg J, Zemb T (2004) Shape control through molecular segregation in giant surfactant aggregates. Proc Natl Acad Sci USA 101:15082–15087

Egeblad M, Nakasone E, Werb Z (2010) Tumors as organs: complex tissues that interface with the entire organism. Dev Cell 18:884–901

Falcone J, Chopard B, Hoekstra A (2010) MML: towards and multiscale modeling language. Procedia Comput Sci 1:819–826

Fearon E, Volgestein B (1990) A genetic model for colorectal tumorigenesis. Cell 61:759–767

Fevr T, Robine S, Louvard D, Huelsken J (2007) Wnt/beta-catenin is essential for intestinal homeostasis and mainteinance of intestinal stem cells. Mol Cell Biol 27:7551–7559

Fischer I et al (2005) Angiogenesis in gliomas: biology and molecular pathophysiology. Brain Pathol 15:297–310

Fotos J et al (2006) Automated time-lapse microscopy and high-resolution tracking of cell migration. Cytotechnology 51:7–19

Frank S (2007) Dynamics of cancer. Princeton University Press, Princeton

Free S et al (2005) Notch signals control the fate of immature progenitor cells in the intestine. Nature 435:964–968

Freyer J, Sutherland R (1986) Regulation of growth saturation and development of necrosis in emt6/ro multicellular spheroids by the glucose and oxygen supply. Cancer Res 46:3504–3512

Galiatsatos P, Foulkes W (2006) Familial adenomatous polyposis. Am J Gastroenterol 101:385–398

Galle J, Aust G, Schaller G, Beyer T, Drasdo D (2006) Individual cell-based models of the spatial-temporal organization of multicellular systemsóachievements and limitations. Cytometry Part A 69A(7): 704–710. doi:10.1002/cyto.a.20287

Galle J, Hoffmann M, Aust G (2009) From single cells to tissue architecture: a bottom-up approach to modelling the spatio-temporal organisation of complex multi-cellular systems. J Math Biol 58:261–283. doi:10.1007/s00285-008-0172-4

Galle J, Loeffler M, Drasdo D (2005) Modeling the effect of deregulated proliferation and apoptosis on the growth dynamics of epithelial cell populations in vitro. Biophys J 88:62–75. doi:10.1529/biophysj.104.041459

Galle J, Sittig D, Hanisch I, Wobus M, Wandel E, Loeffler M, Aust G (2006) Individual cell-based models of tumor-environment interactions: multiple effects of CD97 on tumor invasion. Am J Pathol 169(5):1802–1811 doi:10.2353/ajpath.2006.060006

Gene Ontology Consortium (2006) The gene ontology (GO) project in 2006. Nucleic Acid Res (Database issue) 34:D322–D326

Gerike T, Paulus U, Potten C, Loeffler M (1998) A dynamic model of proliferation and differentiation in the intestinal crypt based on a hypothetical intraepithelial growth factor. Cell Prolif 31:93–110. http://www.ncbi.nlm.nih.gov/pubmed/9745618

Gibson MA, Bruck J (2000) Efficient exact stochastic simulation of chemical systems with many species and many channels. J Phys Chem 104:1876–1889

Gierer A et al (1972) Regeneration of hydra from reaggregated cells. Nat New Biol 91:98–101

Gierer A, Meinhardt H (1974) Biological pattern formation involving lateral inhibition. Lect Math Life Sci 7:163–183

Gillespie DT (1976) A general method for numerically simulating the stochastic time evolution of coupled chemical reactions. J Comput Phys 22:403–434

Gillespie DT (1977) Exact stochastic simulation of coupled chemical reactions. J Phys Chem 2340–2361

Glauche I, Cross M, Loeffler M, Roeder I (2007) Lineage specification of hematopoietic stem cells: Mathematical modeling and biological implications. Stem cells 25:1791–1799

Goss K, Groden J (2000) Biology of the adenomatous polyposis coli tumor suppressor. J Clin Oncol 18:1967–1979

Graner F, Glazier J (1992) Simulation of biological cell sorting using a two-dimensional extended potts model. Phys Rev Lett 69:2013–2017

Graner F, Glazier J (1993) Simulation of the differential adhesion driven rearrangement of biological cells. Phys Rev E 47:2128–2154. http://graner.net/francois/publis/glazier_rearrangement.pdf

Graudenzi A, Caravagna G, De Matteis G, Mauri G, Antoniotti M (2012) A multiscale model of intestinal crypts dynamics. In: Proceedings of the Italian Workshop on Artificial Life and Evolutionary Computation, WIVACE 2012. ISBN: 978-88-903581-2-8
Greenberg J, Hassard B, Hastings S (1978) Pattern formation and periodic structures in systems modeled by reaction-diffusion equations. Bull Am Math Soc 84:1296–1327
Gregorieff A, Pinto D, Begthel H, Destree O, Kielman M, Clevers H (2005) Expression pattern of wnt signaling components in the adult intestine. Gastroenterology 129:626–638
Grindrod P (1991) Patterns and waves: theory and applications of reaction–diffusion equations. Oxford Applied Mathematics & Computing Science, Oxford
Hafner C et al (2005) Ephrin-b2 is differentially expressed in the intestinal epithelium in crohn's disease and contributes to accelerated epithelial wound healing in vitro. World J Gastroenterol 11:4024–4031
Haga H et al (2005) Collective movemente of epithelial cells on a collagen gel substrate. Biophys J 88: 2250–2256
Hanahan D, Folkman J (1996) Patterns and emerging mechanisms of the angiogenetic switch during tumorigenesis. Cell 86:353–364
Hanahan D, Weinberg RA (2011) Hallmarks of cancer: the next generation. Cell 144:646–674
Harrison NC (2010) BioCellSim 1.0 Simulation Software. http://pcwww.liv.ac.uk/~mf0u4027/biocellsim.html
Hartsock A, Nelson W (2007) Adherens and tight junctions: structure, function and connections to the actin cytoskeleton. Biochim Biophys Acta. doi:10.1016/j.bbamem.2007.07.012
Haselwandter CA, Phillips R (2011) Elastic energy of polyhedral bilayer vesicles. Phys Rev E 83(6):061,901. doi:10.1103/PhysRevE.83.061901
Heckera M et al (2009) Gene regulatory network inference: data integration in dynamic models—a review. Biosystems 96:86–103
Hocker M, Wiedenmann B (1998) Molecular mechanisms of enteroendocrine differentiation. Ann NY Acad Sci 859:160–174
Hoehme S, Drasdo D (2010) A cell-based simulation software for multicellular systems. Bioinformatics 26(20):2641–2642
Hogeweg P (2000) Evolving mechanisms of morphogenesis: on the interplay between differential adhesion and cell differentiation. J Theor Biol 203(4):317–333. doi:10.1006/jtbi.2000.1087
Hogeweg P (2002) Computing an organism: on the interface between informatic and dynamic processes. Biosystems 64(1-3):97–109. doi:10.1016/S0303-2647(01)00178-2
Holmberg J et al (2006) Ephb receptors coordinate migration and proliferation in the intestinal stem cell niche. Cell 125:1151–1163
Honda H, Yamanaka H, Eguchi G (1986) Transformation of a polygonal cellular pattern during sexual maturation of the avian oviduct epithelium. J Embryol Exp Morphol 98:1–19
Huynh-Do U, Stein E, Lane AA, Liu H, Cerretti DP, Daniel TO (1999) Surface densities of ephrin-b1 determine ephb1-coupled activation of cell attachment through avb3 and a5b1 integrins. EMBO J 18:2165–2173
Ikushima H, Miyazono K (2010) Tgfbeta signaling: a complex web in cancer progression. Nat Rev Cancer 10:415–424
Ireland H, Houghton C, Howard L, Winton D (2005) Cellular inheritance of a cre-activated reporter gene to determine paneth cell longevity in the murine small intestine. Dev Dyn 233:1332–1336
Jass JR (2007) Classification of colorectal cancer based on correlation of clinical, morphological and molecular features. Histopathology 50:113–130
Jass JR, Whitehall VL, Young J, Leggett BA (2002) Emerging concepts in colorectal neoplasia. Gastroenterology 123:862–876
Jass JR, Young J, Leggett BA (2002) Evolution of colorectal cancer: change of pace and change of direction. J Gastroenterol Hepatol 17:17–26
Jemal A, Siegel R, Xu J, Ward E (2010) Cancer statistics 2010. CA Cancer J Clin 60:277–300
Jensen U, Lowell S, Watt F (1999) The spatial relationship between stem cells and their progeny in the basal layer of human epidermis: a new view based on whole-mount labelling and lineage analysis. Development 126:2409–2418
Jouanneau J, Tucker G, Boyer B, Vallés AJPT (1992) Epithelial cell plasticity in neoplasia. Cancer Cells 3:525–529
Kaneko K (2006) Life: an introduction to complex systems biology. Springer, Berlin
Kauffman S (1969) Homeostasis and differentiation in random genetic control networks. Nature 224:177

Kauffman S (1969) Metabolic stability and epigenesis in randomly constructed genetic nets. J Theor Biol 22:437–467
Kauffman S (1995) At home in the universe. Oxford University Press, Oxford
Kaur P, Potten C (1986) Circadian variation in migration velocity in small intestinal epithelium. Cell Tissue Kinet 19:591
Kedinger M et al (1986) Fetal gust menschyme induces differentiation of cultured intestinal endonormal and crypt cells. Dev Biol 113:474–483
Kempf H, Bleicher M, Meyer-Hermann M (2010) Spatio-temporal cell dynamics in tumour spheroid irradiation. Eur Phys J D 60(1):177–193
Kinzler KW, Vogelstein B (1996) Lessons from hereditary colorectal cancer. Cell 87:159–170
Kinzler KW, Vogelstein B (2002) Colorectal tumors. In: Vogelstein B, Kinzler KW (eds) The genetic basis of human cancer, 2nd edn. McGraw-Hill, New York
Kirouac D, Ito C, Csaszar E, Roch A, Yu M, Sykes E, Bader G, Zandstra P (2010) Dynamic interaction networks in a hierarchically organized tissue. Mol Syst Biol 6:417
Kitano H (2001) Foundations of systems biology. MIT Press, Massachusetts
Kitano H (2002) Computational systems biology. Nature 206–210
Koga S, Kuramoto Y (1980) Localized patterns in reaction-diffusion systems. Prog Theor Phys 63:106–121
Köhn D, Novère NL (2008) SED-ML - An XML Format for the Implementation of the MIASE Guidelines. In: Computational methods n systems biology. Lncs, vol. 5307. Springer, Berlin, pp 176–190
Kohn K (1998) Functional capabilities of molecular network components controlling the mammalian g1/s cell cycle phase transition. Oncogene 16:1065–1075
Koinuma K, Shitoh K, Miyakura Y et al (2004) Mutations of braf are associated with extensive hmlh1 promoter methylation in sporadic colorectal carcinomas. Int J Cancer 108:237–242
Komarova N, Sengupta A, Nowak M (2003) Mutation-selection networks of cancer initiation: tumor suppressor genes and chromosomal instability. J Theor Biol 223:433–450. doi:10.1016/S0022-5193(03)00120-6
Komarova N, Wang L (2004) Initiation of colorectal cancer: where do the two hits hit?. Cell Cycle 3:1558–1565. doi:10.4161/cc.3.12.1186
Komarova N, Wodarz D (2004) The optimal rate of chromosome loss for the inactivation of tumor suppressor genes in cancer. Proc Natl Acad Sci USA 101:7017–7021. doi:10.1073/pnas.0401943101
Korinek V, Barker N, Moerer P, van Donselaar E, Huls G et al (1998) Depletion of epithelial stem-cell compartments in the small intestine of mice lacking tcf-4. Nat Genet 19:379–383
Kosinski C, Li V, Chan A, Zhang J, Ho C, Tsui W et al (2007) Gene expression patterns of human colon tops and basal crypts and bmp antagonists as intestinal stem cell niche factors. Proc Natl Acad Sci USA 104:15418–15423
Kullander K, Klein R (2002) Mechanisms and functions of eph and ephrin signaling. Nat Rev Mol Cell Biol 3:475–486
Kunz-Schughart L et al (2000) Proliferative activity and tumorigenic conversion: impact on cellular metabolism in 3-d culture. J Physiol Cell Physiol 278:765
Laird D (1996) The life cycle of a connexin: gap junction formation, removal, and degradation. J Bioenerg Biomembr 28:311–318
Landry J, Freyer J, Sutherland R (1981) Shedding of mitotic cells from the surface of multicell spheroids during growth. J Cell Physiol 106:23–32
Le Novère N, Bornstein B, Broicher A, Courtot M, Donizelli M, Dharuri H, Li L, Sauro H, Schilstra M, Shapiro B, Snoep JL, Hucka M (2006) BioModels Database: a free, centralized database of curated, published, quantitative kinetic models of biochemical and cellular systems. Nucleic Acids Res 34(Database issue):D689–D691
Lee T et al (2002) Transcriptional regulatory networks in *Saccharomyces cerevisiae*. Science 298:799–804
Lemmon M, Schlessinger J (2010) Cell signaling by receptor tyrosine kinases. Cell 141:1117–1134
Lewis J (1998) Notch signalling: a short cut to the nucleus. Nature 393:304–305
Li C, Donizelli M, Rodriguez N, Dharuri H, Endler L, Chelliah V, Li L, He E, Henry A, Stefan MI, Snoep JL, Hucka M, Le Novère N, Laibe C (2010) BioModels database: an enhanced, curated and annotated resource for published quantitative kinetic models. BMC Syst Biol 4:92
Li Y et al (1994) The crypt cycle in mouse small intestinal epithelium. J Cell Sci 107:3271–3279
Lin G, Xu N, Xi R (2008) Paracrinewingless signalling controls selfrenewal of drosophila intestinal stem cells. Nature 455:1119–1123

Loeffler M, Potten C, Paulus U, Glatzer J, Chwalinski S (1988) Interstinal crypt proliferation. II. Computer modeling of mitotic index data provides further evidence for lateral and vertical cell migration in the absence of mitotic activity. Cell Tissue Kinet 21:247–258
Loeffler M, Stein R, Wichmann H, Potten C, Kaur P, Chwalinski S (1986) Intestinal cell proliferation. I. A comprehensive model of steady-state proliferation in the crypt. Cell Tissue Kinet 19:627–645
Logan C, Nusse R (2004) The wnt signaling pathway in development and disease. Annu Rev Cell Dev Biol 20:781–810
Lopez-Garcia CA, Klein M, Simons B, Winton D (2010) Intestinal stem cell replacement follows a patter of neutral drift. Science 330:822–825
Lowell S et al (2000) Stimulating of human epidermal differentiation by delta–notch signalling at the boundaries of stem-cells clusters. Curr Biol 10:491–500
Luebeck E, Moolgavkar S (2002) Multistage carcinogenesis and the incidence of colorectal cancer. Proc Natl Acad Sci USA 99:15095–15100. doi:10.1073/pnas.222118199
Macklin P et al (2009) Multiscale modeling and nonlinear simulation of vascular tumour growth. J Math Biol 58:765–798
Macklin P, Edgerton M, Thompson A, Cristini V (2010) MultiCellXML: an open XML data standard for multicell agent models. http://multicellxml.sourceforge.net
Multiscale Applications on European e-Infrastructures (2010) http://www.mapper-project.eu
Mardis E (2008) The impact of next-generation sequencing technology on genetics. Trends Genet 24:133–141
Marshman E, Booth C, Potten C (2002) The intestinal epithelial stem cells. Bioessays 24:91–98
Marshman F et al (2001) Caspase activation during spontaneous and radiation-induced apoptosis in the murine intestine. J Pathol 195:285–292
Martiel JL, Goldbeter A (1987) A model based on receptor desensitization for cyclic amp signaling in dictyostelium cells. Biophys J 52:807–828. doi:10.1016/S0006-3495(87)83275-7
Martone ME, Tran J, Wong WW, Sargis J, Fong L, Larson S, Lamont SP, Gupta A, Ellisman MH (2008) The Cell Centered Database project: an update on building community resources for managing and sharing 3D imaging data. J Struct Biol 161(3):220–231
Mathew JP, Taylor BS, Bader GD, Pyarajan S, Antoniotti M, Chinnaiyan AM, Sander C, Burakoff SJ, Mishra B (2003) From bytes to bedside: data integration and computational biology for translational cancer research. PLoS Comput Biol 102(18): 6245–6250. doi:10.1371/journal.pcbi.0030012
McClay D, Ettensohn C (1987) Cell adhesion in morphogenesis. A. Rev Cell Biol 3:319–345
Medema JP, Vermulen L (2011) Microenvironmental regulation of stem cells in intestinal homeostasis and cancer. Nature 474(7351):318–326
Meineke F, Potten C, Loeffler M (2001) Cell migration and organization in the intestinal crypt using a lattice-free model. Cell Prolif 34(4):253–266
Meinhardt H, Gierer A (1974) Applications of a theory of biological pattern formation based on lateral inhibition. J Cell Sci 15:321–346
Merks RM, Brodsky SV, Goligorksy MS, Newman SA, Glazier JA (2006) Cell elongation is key to in silico replication of in vitro vasculogenesis and subsequent remodeling. Dev Biol 289(1):44–54. doi:10.1016/j.ydbio.2005.10.003
Merks RM, Glazier JA (2005) A cell-centered approach to developmental biology. Phys A Stat Mech Appl 352(1):113–130. doi:10.1016/j.physa.2004.12.028
Miao H, Burnett E, Kinch M, Simmon E, Wang B (2000) Activation of epha2 kinase suppresses integrin function and causes focal-adhesion-kinase dephosphorylation. Nat Cell Biol 2:62–69
Miao H, Strebhardt K, Pasquale E, Shen T, Guan J, Wang B (2005) Inhibition of integrin-mediated cell adhesion but not directional cell migration requires catalytic activity of ephb3 receptor tyrosine kinase. role of rho family small gtpases. J Biol Chem 2:923–932
Michaelis L, Menten M (1913) Die Kinetik der Invertinwirkung. Biochemische Zeitschrift 49:333–369
Mombach J, de Almeida R, Iglesias J (1993) Mitosis and growth in biological tissues. Phys Rev E 48:598
Monk N, Owen M (2011) http://www.cellsignet.org.uk/multicellular2011/
Morel D, Marcelpoil R, Brugal G (2001) A proliferation control network model: The simulation of two-dimensional epithelial homeostasis. Acta Biotheoretica 49:219–234. doi:10.1023/A:1014201805222
Mumm J, Kopan R (2000) Notch signaling: from the outside in. Dev Biol 228:151–165
Munemitsu S, Albert I, Souza B, Rubinfeld B, Polakis P (1995) Regulation of intracellular beta-catenin levels by adenomatous polyposis coli (apc) tumor-suppressor protein. Proc Natl Acad Sci USA 92:3046–3050

Nicol A, Garrod D (1979) The sorting out of embryonic cells in monolayer, the differential adhesion hypothesis and the non-specificity of cell adhesion. J Cell Sci 38:249–266
Nicol A, Garrod D (1982) Fibronectin, intercellular junctions and the sorting-out of chick embryonic tissue cells in monolayer. J Cell Sci 54:357–372
Nowak M, Komarova N, Sengupta A, Jallepalli P, Shih I, Vogelstein B, Lengauer C (2002) The role of chromosomal instability in tumor initiation. Proc Natl Acad Sci USA 99:16226–16231. doi:10.1073/pnas.202617399
Nowak M, Michor F, Iwasa Y (2003) The linear process of somatic evolution. Proc Natl Acad Sci USA 100:14966–14969. doi:10.1073/pnas.2535419100
Nowak MA, Komarova NL, Sengupta A, Jallepalli PV, Shih I, Vogelstein B, Lengauer C (2002) The role of chromosomal instability in tumor initiation. Proc Natl Acad Sci USA 99:16226–16231
Nucci M, Robinson C, Longo P, Campbell PSRH (1997) Phenotypic and genotypic characteristics of aberrant crypt foci in human colorectal mucosa. Hum Pathol 28:1396–1407
Oki E, Oda S, Maehara Y, Sugimachi K (1999) Mutated gene-specific phenotypes of dinucleotide repeat instability in human colorectal carcinoma cell lines deficient in dna mismatch repair. Oncogene 18:2143–2147
Olson E et al (2006) Gene regulatory networks in the evolution and development of the heart. Science 313:1922
Othmer H, Pate E (1980) Scale-invariance in reaction-diffusion models of spatial pattern formation. Proc Natl Acad Sci USA 77:4180–4184
Pasquale E (2005) Eph receptor signalling casts a wide net on cell behaviour. Nat Rev Mol Cell Biol 6:462–475
Paulus U, Loeffler M, Zeidler J, Owen G, Potten CS (1993) The differentiation and lineage development of goblet cells in the murine small intestinal crypt: experimental and modelling studies. J Cell Sci 106:473–483
Paulus U, Potten C, Loeffler M (1992) A model of the control of cellular regeneration in the intestinal crypt after perturbation based solely on local stem cell regulation. Cell Prolif 25:559–578. doi:10.1111/j.1365-2184.1992.tb01460.x
Peixoto T, Drossel B (2009) Noise in random boolean networks. Phys Rev E 79:036108–036117
Pinto D, Gregorieff A, Beghtel H, Clevers H (2003) Canonical wnt signals are essential for homeostasis of the intestinal epithelium. Genes Dev 17:1709–1713
Pitt-Francis J, Pathmanathan P, Bernabeu MO, Bordas R, Cooper J, Fletcher AG, Mirams GR, Murray P, Osborne JM, Walter A, Chapman, SJ, Garny A, van Leeuwen IM, Maini PK, Rodrìguez B, Waters, SL, Whiteley JP, Byrne HM, Gavaghan DJ (2009) Chaste: a test-driven approach to software development for biological modelling. Comput Phys Commun 180(12):2452–2471 doi:10.1016/j.cpc.2009.07.019
Poliakov A, Cotrina M, Wilkinson D (2004) Diverse roles of eph receptors and ephrins in the regulation of cell migration and tissue assembly. Dev Cell 7:465–480
Porter E, Bevins C, Ghosh D, Ganz T (2002) The multifaceted paneth cell. Cell Mol Life Sci 59:156–170
Potten C et al (1988) Scoring mitotic activity in longitudinal sections of crypts of the small intestine. Cell Tissue Kinet 21:231
Potten C, Gandara R, Mahida Y, Loeffler M, Wright N (2009) The stem cells of small intestinal crypts: where are they? Cell Prolif 42:731–750
Potten C, Loeffler M (1990) Stem cells: attributes, cycles, spirals, pitfalls and uncertainties. lessons from the crypt. Development 110:1001–1020
Potten C, Morris R (1988) Epithelial stem cells in vivo. J Cell Sci 10:45–62
Potten CS, Booth C, Pritchard DM (1997) The intestinal epithelial stem cell: the mucosal governor. Int J Exp Pathol 78:219–243
Pradal C, Dufour-Kowalski S, Boudon F, Fournier C, Godin C (2008) Openalea: a visual programming and component-based software platform for plant modeling. Funct Plant Biol 35(9, 10):751–760. http://www-sop.inria.fr/virtualplants/Publications/2008/PDBFG08a
Rajagopalan H, Nowak MA, Vogelstein B, Lengauer C (2003) The significance of unstable chromosomes in colorectal cancer. Nat Rev Cancer 3:695–701
Ramakrishnan N, Tadepalli S, Watson LT, Helm RF, Antoniotti M, Mishra B (2010) Reverse engineering dynamic temporal models of biological processes and their relationships. PNAS 107(28):12511–12516
Ratdke F, Clevers H (2005) Self-renewal and cancer of the gut: tho sides of a coin. Science 307:1904–1909

Reid JF, Gariboldi M, Sokolova V, Capobianco P, Lampis A, Perrone F, Signoroni S, Costa A, Leo E, Pilotti S, Pierotti MA (2009) Integrative approach for prioritizing cancer genes in sporadic colon cancer. Genes Chromosom Cancer 48(11):953–962
Reya T, Clevers H (2005) Wnt signalling in stem cells and cancer. Nature 434:843–850
Reya T, Morrison S, Clarke M, Weissman I (2001) Stem cells, cancer, and cancer stem cells. Nature 414:105–111
Roeder I, Braesel K, Lorenz R, Loeffler M (2007) Stem cell fate analysis revisited: Interpretation of individual clone dynamics in the light of a new paradigm of stem cell organization. J Biomed Biotechnol. doi:10.1155/2007/84656
Roeder I, Loeffler M (2002) A novel dynamic model of hematopoietic stem cell organization based on the concept of within-tissue plasticity. Exp Hematol 30:853–861
Rubinfeld B, Robbins P, EL Gamil M, Albert I, Porfiri E, Polakis P (1997) Stabilization of beta-catenin by genetic defects in melanoma cell lines. Science 275:1790–1792
Ruoslahti E (1997) Stretching is good for a cell. Science 276:1345–1346
Saito T, Masuda N, Miyazaki T, Kanoh K, Suzuki H, Shimura T, Asao T, Kuwano H (2004) Expression of epha2 and e-cadherin in colorectal cancer: correlation with cancer metastasis. Oncol Rep 11:605–611
Samson O et al (2004) Loss of apc in vivo immediately perturbs wnt signaling, differentiation and migration. Genes Dev 18:1385–1390
Samuel S, Walsh R, Webb J, Robins A, Potten C, Mahida Y (2009) Characterization of putative stem cells in isolated human colonic crypt epithelial cells and their interactions with myofibroblasts. Am J Physiol Cell Physiol 296:C296–C305
Sancho E, Batlle E, Clevers H (2004) Signaling pathways in intestinal development and cancer. Annu Rev Cell Dev Biol 20:695–723
Sandersius S, Weijer C, Newman T (2011) Emergent cell and tissue dynamics from subcellular modeling of active bio-mechanical processes. Phys Biol 8:045007
Sato T et al (2011) Paneth cells constitute the niche for lgr5 stem cells in intestinal crypts. Nature 469: 415–418
Savill NJ, Hogeweg P (1997) Modelling morphogenesis: from single cells to crawling slugs. J Theor Biol 184(3):229–235. doi:10.1006/jtbi.1996.0237
Savill NJ, Sherratt JA (2003) Control of epidermal stem cell clusters by notch-mediated lateral induction. Dev Biol 258(1):141–153. doi:10.1016/S0012-1606(03)00107-6
System Biology Markup Language (2002) http://www.smb-sbml.org/
Schaff J (2011) SBML Spatial Geometry Extension Proposal. proposal at http://sbml.org
Schaller G, Meyer-Hermann M (2005) Multicellular tumor spheroid in an off-lattice Voronoi-Delaunay cell model. Phys Rev E 71(5):051910. doi:10.1103/PhysRevE.71.051910
Schroder N, Gossler A (2002) Expression of notch pathway components in fetal and adult mouse small intestine. Gene Expr Patterns 2:247–250
Sekimura T, Kobuchi Y (1986) A spatial pattern formation model for dictyostelium discoideum. J Theor Biol 122:325–338
Serini G et al (2003) Modeling the early stages of vascular network assembly. EMBO J 22:1771–1779
Serra R, Villani M, Barbieri A, Kauffman S, Colacci A (2010) On the dynamics of random boolean networks subject to noise: attractors, ergodic sets and cell types. J Theor Biol 265:185–193
Shirinifard A, Gens JS, Zaitlen BL, Poplawski NJ, Swat M, Glazier, JA (2009) 3d multi-cell simulation of tumor growth and angiogenesis. PLoS ONE 4(10):e7190. doi:10.1371/journal.pone.0007190
Siegert F, Weijer C (1992) Three dimensional scroll waves organise dictyostelium slugs. Proc Natl Acad Sci USA 89:6433–6437
Smallwood R, Holcombe W, Walker D (2004) Development and validation of computational models of cellular interaction. J Mol Histol 35:659–665. doi:10.1007/s10735-004-2660-1
Smith B, Ashburner M, Rosse C, Bard J, Bug W, Ceusters W, Goldberg LJ, Eilbeck K, Ireland A, Mungall CJThe OBI Consortium, Leontis N, Rocca-Serra P, Ruttenberg A, Sansone SA, Scheuermann RH, Shah N, Whetzel PL, Lewis S (2007) The OBO Foundry: coordinated evolution of ontologies to support biomedical data integration. Nature Biotechnol 25:1251–1255
Snippert H et al (2010) Intestinal crypt homeostasis results from neutral competition between symmetrically dividing lgr5 stem cells. Cell 143:134–144
Springer W, Barondes S (1978) Direct measurement of species specific cohesion in cellular slime molds. J Cell Biol 79:937–942

Steimberg M, Garrod D (1975) Observations on the sorting-out of embryonic cells in monolayer culture. J Cell Sci 18:385–403
Stein L (2004) Reactome site. http://www.reactome.org
Steinberg M (1962) On the mechanism of tissue reconstruction by dissociated cells. i population kinetics, differential adhesiveness, and the absence of directed migration. Proc Natl Acad Sci USA 48: 1577–1582
Sternfeld J (1979) Evidence for differential cellular adhesion as the mechanism of sorting out of various slime mold species. J Embryol Exp Morphol 53:163–177
Sulsky D, Childress S, Percus JK (1984) A model of cell sorting. J Theor Biol 106(3):275–301. doi:10.1016/0022-5193(84)90031-6
Takeuchi I, Kakutani T, Tasaka M (1988) Cell behavior during formation of prestalk/prespore pattern in submerged agglomerates of dictyostelium discoideum. Dev Genet 9:607–614
Takeuchi I, Tasaka M (1989) Formation of differentiation pattern in dictyostelium discoideum. Genome 31:620–624
Talmadge J, Fidler I (2010) Aacr centennial series: the biology of cancer metastasis: historical perspective. Cancer Res 70:5649–5669
Technau U, Holstein T (1992) Cell sorting during the regeneration of hydra from reaggregated cells. Dev Biol 151:117–127
Tepass U, Godt D, Winklbauer R (2002) Cell sorting in animal development: signalling and adhesive mechanisms in the formation of tissue boundaries. Curr Opin Genet Dev 12:572–582
The Cancer Genome Atlas. http://cancergenome.nih.gov/
Thibodeau S, Bren G, Schaid D (1993) Microsatellite instability in cancer of the proximal colon. Science 260:816–819
Thirlwell C et al (2010) Clonality assessment and clonal ordering of individual neoplastic crypts shows polyclonality of colorectal adenomas. Gastroenterology 138:1441–1454
Thomas W, Yancey J (1988) Can retinal adhesion mechanisms determine cell-sorting patterns: a test of the differential adhesion hypothesis. Development 103:37–48
Toyota M et al (1999) Cpg island methylator phenotype in colorectal cancer. PNAS 96:8681–8686
Tsubouchi S (1983) Theoretical implications for cell migration through the crypt and the villus of labeling studies conducted at each position within the crypt. Cell Tissue Kinet 16:441–456
Turner S, Sherratt JA (2002) Intercellular adhesion and cancer invasion: a discrete simulation using the extended potts model. J Theor Biol 216(1):85–100. doi:10.1006/jtbi.2001.2522
Vajdic C, Leeuwen M (2009) Cancer incidence and risk factors after solid organ transplantation. Int J Cancer 125:1747–1754
van de Wetering M, Sancho E, Verweij C, de Lau W, Oving I et al (2002) The beta-catenin/tcf-4 complex imposes a crypt progenitor phenotype on colorectal cancer cells. Cell 111:241–250
van der Flier L et al (2009) Transcription factor achaete scute-like 2 constrol intestinal stem cell fate. Cell 136:903–912
van der Flier L, Clevers H (2009) Stem cells, self-renewal, and differentiation in the intestinal epithelium. Annu Rev Physiol 71:241–260
van Es J et al (2005) Notch/gamma-secretase inhibition turns proliferative cells in intestinal crypts and adenomas into goblet cells. Nature 435:959–963
van Es J, Jay P, Gregorieff A, van Gijn M, Jonkheer S, Hatzis P et al (2005) Wnt signaling induces maturation of paneth cells in intestinal crypt. Nat Cell Biol 7:381–386
van Es JH, van Gijn ME, Riccio OMv, Vooijs M, Begthel H, Cozijnsen M, Robine S, Winton DJ, Radtke F, Clevers H (2005) Notch/γ-secretase inhibition turns proliferative cells in intestinal crypts and adenomas into goblet cells. Nature 435:959–963. doi:10.1038/nature03659
van Leeuwen IM, Byrne HM, Jensen OE, King JR: Elucidating the interactions between the adhesive and transcriptional functions of [beta]-catenin in normal and cancerous cells. J Theor Biol 247(1):77–102 (2007) doi:10.1016/j.jtbi.2007.01.019
van Leeuwen IMM, Byrne HM, Jensen OE, King JR (2006) Crypt dynamics and colorectal cancer: advances in mathematical modelling. Cell Prolif 39(3):157–181. doi:10.1111/j.1365-2184.2006.00378.x
Villani M, Barbieri A, Serra R (2011) A dynamical model of genetic networks for cell differentiation. PLoS ONE 6(3):e17703. doi:10.1371/journal.pone.0017703
Wagner A (2002) Estimating coarse gene network structure from large-scale gene gene perturbation data. Genome Res 12:309–315

Walker D, Southgate J, Hill G, Holcombe M, Hose D, Wood S, Mac Neil S, Smallwood R (2004) The epitheliome: agent-based modelling of the social behaviour of cells. Biosystems 76(1-3):89–100. doi:10.1016/j.biosystems.2004.05.025
Wang B (2011) Cancer cells exploit the eph-ephrin system to promote invasion and metastasis: tales of unwitting partners. Sci Signal 4(175):128
Wang M, Schaap P (1989) Ammonia depletion and dif trigger stalk cell differentiation in intact dictyostelium discoideum slugs. Development 105:569–574
Wehrle J et al (2000) Metabolism of alternative substrates and the bioenergetic status of emt6 tumor cell spheroids. NMR Biomed 13:349–360
Wilkinson DG (2003) Multiple roles of eph receptors and ephrins in neural development. Nat Rev Neurosci 2:155–164
Winton D, Ponder B (1990) Stem-cell organization in mouse small intestine. Proc Biol Sci 241:13–18
Winton DJ, Blount M, Ponder B (1988) A clonal marker induced by mutation in mouse intestinal epithelium. Nature 333:463–466
Witsch E, Sela M, Yarden Y (2010) Roles for growth factors in cancer progression. Physiology (Bethesda) 25:85–101
Wodarz A (1998) Mechanisms of wnt signaling in development. Annu Rev Cell Dev Biol 14:59–88
Wodarz D, Komarova N (2005) Computational biology of cancer: lecture notes and mathematical modeling. World Scientific Publishing, Hackensack
Wong MH (2004) Regulation of intestinal stem cells. J Invest Dermatol Symp Proc 9:224–228
Wong SY, Chiam KH, Lim CT, Matsudaira P (2010) Computational model of cell positioning: directed and collective migration in the intestinal crypt epithelium. J R Soc Interf 7(Suppl 3):S351–S363. doi:10.1098/rsif.2010.0018.focus
Wright N, Alison M (1984) The biology of epithelial cell populations. Clarendon Press, Oxford
Xu Q, Mellitzer G, Robinson V, Wilkinson D (1999) In vivo cell sorting in complementary segmental domains mediated by eph receptors and ephrins. Nature 399:267–271
Yen T, Wright N (2006) The gastrointestinal tract stem cell niche. Stem Cell Rev 2:203–212
Zheng X, Wise S, Cristini V (2005) Nonlinear simlation of tumor necrosis, neo-vascularization and tissue invasion via an adaptive finite-element/level-set method. Bull Math Biol 67:211–259
Zimmerman W, Weijer C (1993) Analysis of cell cycle progression during the development of dictyostelium and its relationship to differentiation. Dev Biol 160:178–185
Zipori D (2004) The nature of stem cells: state rather than entity. Nat Rev Genet 5:873–878
Zou J, Wang B, Kalo M, Zisch A, Pasquale E, Ruoslahti E (1999) An eph receptor regulates integrin activity through r-ras. Proc Natl Acad Sci 96:13813–13818